



# **Optimization of the Machining Parameters for Ultrasonic Vibration Assisted Turning of Hard Material**



**SUBMITTED BY: GIRIJA NANDAN ARKA**

**GUIDED BY: PROF. S.K.SAHOO**



**ROLL NO: 212ME2291**

**SPECIALISATION:  
PRODUCTION ENGINEERING**

**MECHANICAL ENGINEERING DEPARTMENT**

**NATIONAL INSTITUTE OF TECHNOLOGY,  
ROURKELA-769008**

# **OPTIMIZATION OF THE MACHINING PARAMETERS FOR ULTRASONIC VIBRATION ASSISTED TURNING OF HARD MATERIAL**

*A Thesis Submitted in Partial Fulfillment of the requirements for  
the degree of*

Master of Technology  
In  
Mechanical Engineering

By

*Girija Nandan Arka*  
**212ME2291**



**Department of Mechanical Engineering  
National Institute of Technology Rourkela  
2013-2014**

# **OPTIMIZATION OF THE MACHINING PARAMETERS FOR ULTRASONIC VIBRATION ASSISTED TURNING OF HARD MATERIAL**

*A Thesis Submitted in Partial Fulfillment of the requirements for  
the degree of*

Master of Technology  
In  
Mechanical Engineering

By

**GIRIJA NANDAN ARKA**  
212ME2291

*Under the guidance of*

**Dr. S. K. SAHOO**



**Department of Mechanical Engineering  
National Institute of Technology Rourkela  
2013-2014**



National Institute of Technology

Rourkela (India)

### **CERTIFICATE**

This is to certify that the thesis entitled, “**OPTIMIZATION OF THE MACHINING PARAMETERS FOR ULTRASONIC VIBRATION ASSISTED TURNING OF HARD MATERIAL**” submitted by **Mr. Girija Nandan Arka** having Roll No. **212ME2291** in partial fulfillment of the requirement for the award of the degree of Master of Technology Degree in Mechanical Engineering with specialization in Production Engineering at the National Institute of Technology, Rourkela (Deemed University) is an authentic work carried out by him under my supervision and guidance.

The results presented in this thesis has not been, to the best of my knowledge, submitted to any other University or Institute for the award of any degree or diploma. The thesis, in my opinion, has reached the standards fulfilling the requirement for the award of the degree of Master of technology in accordance with regulations of the Institute.

Date:

**Dr. Susanta Kumar Sahoo**

Professor  
Deptt. of Mechanical Engineering  
National Institute of Technology  
Rourkela

## ACKNOWLEDGEMENT

I express my deep sense of gratitude and indebtedness to my supervisor Dr. S. K. Sahoo, Professor of Department of Mechanical Engineering for his extensive support throughout this project work. His timely help, constructive criticism, and conscientious efforts made it possible to present the work Contained in this thesis. Working under him has indeed been a great experience and inspiration for me.

I am grateful to Prof. K. P. Maity, Head of the Department of Mechanical Engineering for providing me the necessary facilities in the department. I express my sincere thanks to my senior PhD. Scholars Mr. Vivekananda Kukkala and Mr. Mantra Satpathy for his timely help during the course of work. I also thankful to Mr. Kunal sir for carried out the experimental investigation for my research work.

I would like to thank all my friends and especially my classmates for all the thoughtful and mind stimulating discussions we had, which prompted us to think beyond the obvious.

Last but not least I would like to thank my parents, who taught me the value of hard work by their own example. They rendered me enormous support being apart during the whole tenure of my stay in NIT Rourkela

**Place:**

(Girija Nandan Arka)  
Mechanical Engineering -212ME2291  
212me2291@nitrkl.ac.in  
NIT Rourkela

## ABSTRACT

Use of hard material like stainless steel, Inconel 718 etc. has been increased in many industries like aerospace sector, defense sector etc. It has been noticed that hard material are very difficult to cut in conventional turning process. Ultrasonic assisted turning process found to be a good alternative process to cut hard material by giving vibration to the tool and hence it acts as intermittent cutting which leads to increase tool life. In the present work FEM analysis has been done for Horn (acts as amplifier as well as tool holder) using mild steel material to know the frequency and amplitude of vibration at the output end by ANSYS<sup>®</sup> software and has been manufactured. Experimental investigation has been carried out for both conventional turning process and Ultrasonic assisted turning process to know the various process parameter effects on cutting forces and surface finish generated. From the experiment it has been found that Ultrasonic assisted turning improves both cutting force and surface finish. Finally Gray Taguchi method adopted for optimize both cutting force and surface finish (Multi objective optimization) to get the best combination of process parameters.

***Keywords: FEM analysis, Harmonic analysis, Modal analysis, UAT, UVT***

## ABBREVIATIONS

ANOVA	Analysis of variance
ANSYS	Analysis of system
CT	Conventional turning
DAQ	Data acquisitions
FEM	Finite element modeling
GRG	Grey relation grade
Hz	Hertz
MS	Mean square
PC	Personal computer
PZT	Piezoelectric transducer
RAM	Random access memory
SS	Sum of square
UAT	Ultrasonic assisted turning
UVT	Ultrasonic vibratory tool

## NOMENCLATURE

$a$	Amplitude
$C$	Velocity of sound
$D$	Diameter
$d$	Depth of cut
$E$	Young's modulus
$f$	Frequency
$L$	Length
$N$	Spindle speed
$R_a$	Surface roughness
$f$	Feed
$V_c$	Cutting velocity
$V_t$	Velocity of tip
$\lambda$	Wave length
$\xi$	Displacement
$\xi_M$	Maximum displacement
$\rho$	Density
$\omega$	Angular velocity

## LIST OF FIGURE

	Page No
<b>CHAPTER 1</b>	
Figure 1.1 Parts of UAT setup .....	2
Figure 1.2 Mechanism of tool vibration.....	3
Figure 1.3 Different directions of vibration .....	4
<b>CHAPTER 3</b>	
Figure 3.1 Force propagation along the uniform slender bar .....	22
Figure 3.2 Propagation of wave along tapered horn shape .....	24
Figure 3.3 Plane wave propagated through Stepped cylindrical shape.....	25
Figure 3. 4 Stepped horn specification in mm based on 3 <sup>rd</sup> angle of projection .....	28
Figure 3.5 Solid 92 elements represented from ANSYS user guide.....	29
Figure 3.6 Mesh generation of horn assembly .....	30
Figure 3.7 Modal analysis results .....	31
Figure 3.8 Maximum displacement of horn assembly .....	32
Figure 3.9 Displacement vector sum of horn assembly .....	33
Figure 3.10 Stress variation of horn assembly .....	34
Figure 3.11 Strain distributions.....	35
Figure 3.12 Wave propagates in micron amplitude through horn assembly .....	36
<b>CHAPTER 4</b>	
Figure 4.1 Semantic diagram of Experimental set-up of UAT .....	38
Figure 4.2 Rotation of work piece with respect to active edge of cutting tool .....	39
Figure 4. 3 Experimental set-up (a) UAT base, (b) DAQ system connected to amplifier with PC .....	41
Figure 4.4 CT and UAT machined work piece .....	41
Figure 4.5 Graph plotted for 1 <sup>st</sup> run defined in table 4.4.....	44
Figure 4.6 Graph plotted for 2 <sup>nd</sup> run defined in table 4.4.....	45
Figure 4.7 Graph plotted for 3 <sup>rd</sup> run defined in table 4.4 .....	47
Figure 4.8 Graph plotted for 4 <sup>th</sup> run as defined in Table 4.4.....	48
Figure 4.9 Graph plotted for 5 <sup>th</sup> run as defined in Table 4.4.....	49
Figure 4.10 Graph plotted for 6 <sup>th</sup> run as defined in Table 4.4.....	50
Figure 4.11 Graph plotted for 7 <sup>th</sup> run as defined in Table 4.4.....	51
Figure 4.12 Graph plotted for 8 <sup>th</sup> run as defined in Table 4.4.....	52
Figure 4.13 Graph plotted for 9 <sup>th</sup> run as defined in Table 4.4.....	53
Figure 4.14 Comparison of cutting forces for each run defined in Table 4.4 .....	54
Figure 4.15 Comparison of surface roughness for each run defined in Table 4.4 .....	55
<b>CHAPTER 5</b>	
Figure 5.1 Main effects plot for SN ratios of CT GRG .....	59
Figure 5.2 Main effects plot for SN ratios of UAT.....	61



## LIST OF TABLE

	Page No
<b>CHAPTER 1</b>	
Table 2.1 Natural frequency of different horn material [12] .....	11
Table 2.2 Geometrical parameters of sonotrode shapes [17] .....	14
Table 2.3 experimental cutting conditions [20] .....	16
Table 2.4 Fillet radius vs. resonant frequency [24] .....	19
<b>CHAPTER 3</b>	
Table 3.1 Different Horn shape length and magnification factor .....	27
<b>CHAPTER 4</b>	
Table 4.1 Specification of ultrasonic generator .....	40
Table 4.2 Specification of Kistler Dynamometer 9272 .....	40
Table 4.3 Cutting condition for experimentation .....	42
Table 4.4 Experimental results obtained .....	43
<b>CHAPTER 5</b>	
Table 5.1 Finding Gray relational grade (GRG) for CT .....	58
Table 5.2 ANOVA for CT gray relation grade .....	59
Table 5.3 Gray relation grades for UAT .....	60
Table 5.4 ANOVA for UAT Gray relation grade .....	61

# CONTENTS

	Page No
<b>CERTIFICATE</b>	<b>iii</b>
<b>ACKNOWLEDGEMENT</b>	<b>iv</b>
<b>ABSTRACT</b>	<b>v</b>
<b>ABBREVIATIONS</b>	<b>vi</b>
<b>NOMENCLATURE</b>	<b>vi</b>
<b>LIST OF FIGURES</b>	<b>vii</b>
<b>LIST OF TABLE</b>	<b>viii</b>
<b>CHAPTER 1</b>	
<b>1 INTRODUCTION.....</b>	<b>2</b>
1.1 Introduction of UAT .....	2
1.2 Current Needs of Industry.....	6
1.3 Aim and Objective of Research .....	6
1.3.1 Aim of the research .....	6
1.3.2 Objective of the research.....	7
<b>2 LITERATURE REVIEW .....</b>	<b>9</b>
2.1 Summary .....	19
<b>3 HORN DESIGN AND FE ANALYSIS .....</b>	<b>21</b>
3.1 Introduction of Horn .....	21
3.2 Vibratory Tool Equation and its Solution .....	21
3.2.1 Plane wave equation.....	21
3.2.2 Plane wave equation of tapered horn .....	23
3.2.3 The plane wave equation for stepped type shape horn.....	24
3.2.4 Calculation of nodal plane in stepped cylindrical shape horn.....	26
3.3 Finite Element Modeling of Ultrasonic Vibratory tool.....	28
3.3.1 The finite element .....	28
3.3.2 Finite element modeling of horn-tool assembly.....	28
3.4 Result and Analysis of Horn .....	31
3.4.1 Modal analysis .....	31
3.4.2 Harmonic analysis.....	32
3.4.3 Results of FE for horn assembly .....	33
3.5 Conclusion .....	35

<b>4</b>	<b>EXPERIMENTAL INVESTIGATION .....</b>	<b>38</b>
4.1	Experimental Set-up and Description .....	38
4.1.1	Description of the machining process .....	39
4.1.2	Work piece processing .....	40
4.1.3	Cutting force measurement .....	42
4.1.4	Surface roughness measurement .....	42
4.2	Experimental Condition .....	42
4.3	Experimental Results and Discussion .....	42
<b>5</b>	<b>OPTIMIZATION OF MACHINING PARAMETER.....</b>	<b>57</b>
5.1	Design of Experimentation .....	57
5.2	Taguchi Methodology .....	57
5.2.1	Gray relation grade.....	57
5.3	Multi Objective Optimization of CT.....	58
5.3.1	Results and discussion .....	60
5.4	Multi Objective Optimization of UAT.....	60
5.4.1	Result and discussion of UAT .....	61
5.5	Conclusion .....	62
<b>6</b>	<b>CONCLUSIONS AND FUTURE RECOMMENDATIONS .....</b>	<b>64</b>
6.1	Conclusions.....	64
6.2	Future Recommendations .....	65
	<b>REFERENCES.....</b>	<b>67</b>

# **CHAPTER 1**

- **INTRODUCTION OF UAT**
- **CURRENT NEED OF INDUSTRY**
- **AIM AND OBJECTIVE OF RESERCH**

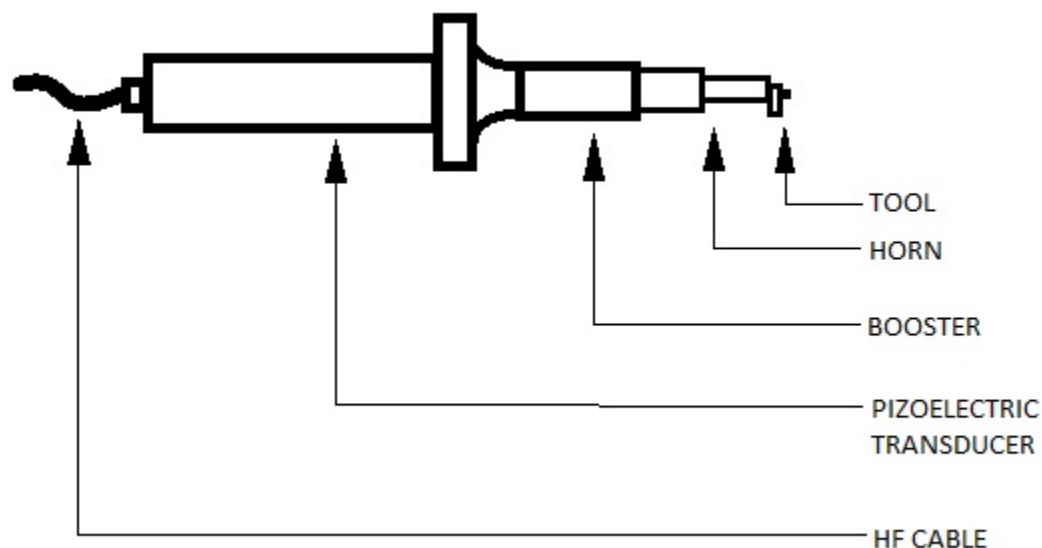
# 1 INTRODUCTION

---

## 1.1 Introduction of UAT

Ultrasonic, which is a specific branch of acoustics deals with vibratory waves in sounds, liquids and gases at frequencies above those within the hearing range of average person and it is at frequencies above 16 kHz. Ultrasonic assisted turning is a non-conventional turning process which acts as an intermittent cutting by giving ultrasonic sound in the form of vibration to the tool tip at a frequency of 20 kHz and 104 micron amplitude.

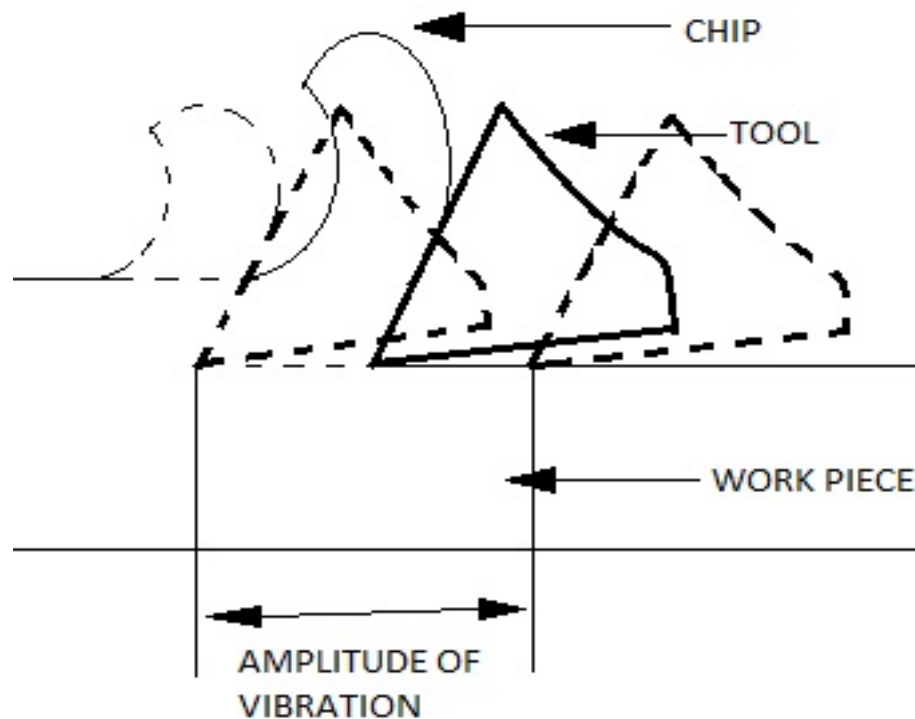
The UAT process consists of piezoelectric transducer, booster, horn and tool as shown in Figure 1.1. In piezoelectric transducer piezoelectric material like quartz is used. In piezoelectric material, quartz, if we supply electrical energy than it will try to deform and produce mechanical energy in the form vibration of required frequency and amplitude of vibration. So in order to amplify the amplitude, booster has been used. In UAT setup we can't use cutting tool in booster, for that horn being used. Horn acts as tool holder as well as an amplifier.



**Figure 1.1** Parts of UAT setup

In any machining process our main motive is to get reduced cutting force and power consumption for increasing tool life and to get a better surface finish for an output machined product. It has been seen that both tool life increased (because of less force and power consumption) and better surface finish has been found in the ultrasonic assisted turning process.

Because of its pulse like cutting, that means some fraction of time (half of the amplitude of vibration) will be contacted with the work piece where cutting operation will be done and another fraction of time it will not contact with the work piece, on that fraction of time cooling process has been done so as a result we can get the reduced force and power consumption which enhance increasing tool life [1-2] as shown in Figure 1.2. So we can conclude that UAT is a better alternative machining process for cutting hard material which is difficult to cut like Inconel 718, Ti alloy, and stainless steel.



**Figure 1.2** Mechanism of tool vibration

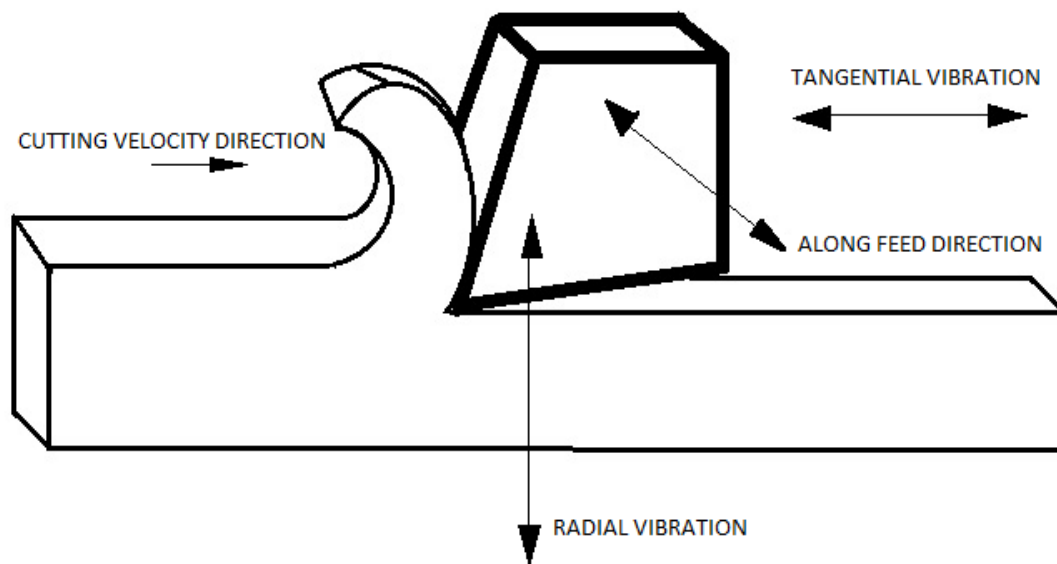
With the growing demand of machining hard material in the aerospace industry, ultrasonic assisted turning has been shown remarkable excellent result as compared to conventional turning. Ultrasonic not only use for turning process, but also used for many operations like ultrasonic drilling, ultrasonic milling, ultrasonic welding, ultrasonic cleaning, etc. It has been seen that ultrasonic process has chatter suppressing dynamics (M. Xiao and K. Sato) [3]. These important characteristics give possible advantages of the ultrasonic technology for industrial machining. The present research is particularly focused on ultrasonic vibration-assisted turning (UAT).

Ultrasonic linear vibration can be given to the tool tip in three possible directions as shown in Figure 1.3 namely

1. Tangential direction of vibration
2. Radial direction of vibration
3. Along feed direction of vibration

In the tangential direction of vibration as shown in the Figure 1.3, the direction of vibration given along the cutting velocity. In this way of vibrating the tool tip is machined into the workpiece at a point. So as a result, we can get a smooth surface of workpiece and reduced cutting force enhancing increasing tool life [4,9].

But in the radial direction of vibration, vibration given in the radial direction as shown in Figure 1.3. Here the cutting force reduced a little bit, but increase the thrust force because of impact action along the radial direction and it will affect the surface finish detrimentally. So it is not suitable to use in radial direction. Similarly, in the feed direction of vibration, the vibration given in the feed direction. In this technique cutting force reduced, but it has had some rubbing action to the machined surface when retracted. So it's also not advisable to use. Finally, among all tangential vibration giving good result.



**Figure 1.3** Different directions of vibration

There is an essential condition is required for the tangential vibration cutting process. In Tangential direction or along cutting velocity:  $V_c = \frac{\pi ND}{60} < V_t = 2\pi af$  1.1

Where  $V_c$  is cutting velocity

$N$  is r.p.m. of spindle

$D$  is the diameter of workpiece in meter

$V_t$  is vibration velocity

$a$  is amplitude of vibration

$f$  is frequency of vibration

The vibration velocity  $2af$  should be greater than the cutting velocity  $\pi ND$ . A rheological model of ultrasonic vibration cutting had been predicted and ensuing experiments confirmed and a evident reduction in the cutting force for UAT by vibration in the tangential direction at a frequency  $f=20$  kHz and amplitude of vibration  $a=10$   $\mu\text{m}$  [2]. An experimental result had been shown by Astashev and Babitsky [5]. According to their experimental results, at higher cutting speed, the cutting force reduced considerably, but after overreaching certain speed ( $V_c > V_t$ ), the vibration didn't affect the figure of the cutting force. The summary of their experiment was that if the cutting force exceeding vibration speed, vibration doesn't have any role to do.

The mechanism of chip form in UAT process is shearing and tearing. When the tooltip comes in contact with the work piece, the layer of the workpiece material is started deforming plastically and try to slide over the tool face producing shear stress on the layer of workpiece material. On further application of the force by the tool tip the shear stresses induced in the layer of material increasing continuously, at some point the shear stress becomes greater than or equal to the ultimate shear stress of working material so that shearing or cracking is started taking place at the tooltip and is propagating towards the surface producing shear plane and separating the chip. Because of lower toughness the shear wave or energy wave at the lower side of chip propagated towards the upper surface, then after the tool tip retracted back by the amplitude of vibration, at this time period chip or work piece does not make any contact and gets cool by



coolant or by air and hence discontinuous chip formed and no chance of built of edge (BUE) formation and hence chips are thin, smooth and long [6-8, 11].

In turning process another essential setup is required. The tip of the tool should be in center line for better machining process. If the tooltip above the center line, the tool simply rubs the work piece without cutting and will produce unwanted sound. If the tool tip below the center line than higher cutting force produced as compared to normal operation. So it is an essential condition that the tool tip should be at center line.

## **1.2 Current Needs of Industry**

It has been seen that the use of hard and brittle material like Inconel, Stainless steel, etc. increasing incredibly in the aerospace industry, petrochemical industry and the nuclear industry because of its excellent mechanical properties at low and intermediate temperature. We know that hard materials are very difficult to cut in conventional machining process because of the immense amount of temperature generation of the tool tip. This high temperature generation leads to form BUE (built of edge) on tool tip and hence damage the tool rake face, that steers damage of the surface finish and produce unwanted sound, chatter and increasing cutting force consumption. The use of ultrasonic on tool tip improves not only decrease the cutting force, but also improve surface quality and hence this process, increase tool life, Because UAT process is an intermittent cutting process and of Vibro-impact action of tool tip onto the work piece.

## **1.3 Aim and Objective of Research**

### **1.3.1 Aim of the research**

The current research aims to gain the technical concept of ultrasonic assisted turning process. The principle of working and the different advantages of ultrasonic assisted turning process. It has been observed that the horn is a vital part of UAT process and the natural frequency and amplitude of vibration not only depends on the shape of the horn but also depends on the material of the horn. So the research aims to know the different shape available and the design and development of the horn using FEM (finite element analysis). The FEM analysis consists of modal analysis and harmonic analysis of horn of specific shape of mild steel material has been taken. Turning of stainless steel work-piece material using both conventional turning process and ultrasonic assisted turning process and analyzing the results in terms of cutting force

and surface finish. Finally the machining parameter or process parameter optimized by Taguchi design.

### **1.3.2 Objective of the research**

1. Study of different shape of horn available
2. FEM analysis in terms of modal analysis and harmonic analysis of horn tool assembly
3. Design of experimental setup for experimentation of stainless steel work piece material
4. Experimental investigation of UAT and conventional turning by using stainless steel work piece material
5. Comparing result in terms of cutting force and surface finish produced on work piece for conventional turning and ultrasonic assisted turning
6. Optimization of process parameter of UAT to get less force induced and better surface finish
7. Depending on the results extracting conclusion

# **CHAPTER 2**

- **LITERATURE REVIEW**
- **SUMMARY**

## 2 LITERATURE REVIEW

---

N. Ahmed et al. [9] had done experimentally study and computation analysis (FEM) of both conventional turning and ultrasonic assisted turning by taking ages INCONEL 718 as work piece material. For the test they had used to cut speed in the range of 5-16 m/min, depth of cut 0.1-0.3 mm, feed rate 0.03-0.1 mm/rev. From their experiment as they conclude that the frequency of vibration increasing from 10 to 30 kHz, the average cutting force decrease by 47%, that means higher the amplitude of vibration or by higher the frequency of vibration decreasing the average cutting force. They also analyzed the effect of vibration on the tool in a tangential direction and feed direction. According to their analysis the tangential vibration had given lower cutting force as compared to feeding direction of vibration which means tangential vibration had given the better result. The UAT had induced highest peak cutting force but decreased the average cutting force as compared to conventional turning.

A review on UAT had been done by V. S. Sharma et al. [10]. They collected the advantages and disadvantages of ultrasonic assisted turning (UAT). According to their review the following advantages had been collected. In UVC due to its lower abrasive wear effect leads to lower the tool flank wear as compared to conventional turning. In UAT, because of its intermittent cutting action wear rate increases very slowly or tool wear acceleration is very low as compared to conventional turning. UAT induces a low cutting force as compared to conventional turning and if machining done on lubricating condition, the cutting force further decreases. UAT improves the machined surface finish as BUE formation is very negligible at a lower feed rate. UAT can also be used for nano-finishing surface quality where  $R_a < 1 \mu\text{m}$  to achieve. UAT lower the cutting force as increasing either frequency of vibration or amplitude of vibration which promote the accuracy of cutting process. Increasing cutting speed in UAT process the cutting force goes on increases as it approaches the critical value and hence vibration velocity at the tip should not exceed the critical value.

Apart from the advantages it has some disadvantage [10]. The disadvantage is the initial high set-up cost, mechanical property of vibration system changes as fitting of different tool holder, tool tip, screw to be adjusted to match the natural frequency. High rigidity tool post or base is needed for UAT process.

A theoretical study had done by establishing the role of tool-workpiece contact ratio by C. Nath and M. Rahman [11]. An experiment had conducted by them by taking Inconel 718 as workpiece material and CBN as tool material and the effect of cutting parameters on machining process was investigated by applying ultrasonic vibration superimposing on the tool tip. They investigated the effect of cutting parameters on the output parameters as cutting force component, surface roughness, tool flank wear width and chip formation. Based on their experimental result and theoretical study, they tried to gather the conclusion by comparing both conventional turning and ultrasonic assisted turning. According to their conclusion made, in the UVC process the machined quality depends on two important factors, namely tool-workpiece contact ratio (TWCR) and tool-workpiece relative speed (TWRS). The TWCR depends on three independent input parameters, namely the frequency of vibration, the amplitude of vibration and the workpiece cutting speed. TWCR (tool-workpiece contact ratio) should be kept as low as possible to get high quality machining and its value is lowered by increasing both amplitude and frequency of vibration and decreasing the workpiece cutting speed. According to their results obtained, the tool flank wear found to be about 12-25% reduced at 10 m/min cutting speed as compared to conventional turning. However, beyond 10 m/min cutting speed due to consecutive high impact action between the tool and workpiece with high tool workpiece contact ratio CBN tool catastrophically failed which is fast wear rate. Hence we can conclude that UAT method is a suitable technique for high surface quality of hard material like Inconel 718 by keeping low cutting speed.

We know that for ultrasonic assisted process horn or tool holding device plays a vital role in machining process because it not only acts as a tool holding device but also to amplify the amplitude of vibration. So a FEM analysis of the horn had done by S. Amini et al. [12] for three types of horn namely cylindrical horn with long and eccentric tool holder, cylindrical horn with concentric tool insert and conical-cylindrical horn with concentric tool insert by using ANSYS® software. For their analysis they had taken three materials namely Inconel 718, AL7075 and Ck 45 as workpiece material and aluminum as horn material. Table 2.1 shows their FEM result.

**Table 2.1** Natural frequency of different horn material [12]

Horn configuration	Material	Length in mm	Frequency in Hz
Cylindrical with eccentric tool holder	aluminum	120	20,415
	steel		20,083
Cylindrical with concentric tool insert	aluminum	125	20,091
	steel	120	20,526
Conical-cylindrical with concentric tool insert	aluminum	110	20,527
	Steel		20,192

They had done FE simulations to investigate the influence of tool's clearance, rake angle, cutting speed and amplitude of vibration on cutting force and stresses acting on Inconel 738 workpiece. According to their conclusion made, In the UAT process the cutting force and stress on workpiece vary periodically and the outputs are significantly less as compared to conventional turning. In UAT the cutting force depends heavily on cutting speed as the cutting speed increases than cutting force go on increases. The effect of tool rake angle has an inverse effect, but the clearance angle has insignificant effects. Among three types of horn, aluminum horn with Conical-cylindrical shaped with concentric tool insert had delivered much more satisfactory performance. The horn should design in such a way that, for its natural frequency to ensure at least one natural frequency occurs within the allowable frequency range.

Another FEM analysis of UAT had done by A. V. Mitofanov et al. [13]. They studied the stress distribution in the cutting region for conventional turning and different stages of the cycle of vibration for ultrasonic assisted turning. The stress state for UAT changes regularly within a cycle of vibration and peak values of stresses attained only during this period as a result the overall force acting on the tool and consequently average cutting forces were approximately three times smaller for ultrasonic assisted turning. The temperature distribution was also analysed by them. According to their analysis the cutting tool temperature was nearly two times smaller for Ultrasonic assisted turning as compared to conventional turning due to reduced time of thermal conductance of the tool as it was intermittent cutting. The simulated residual strains in the machined layer showing 20% lower value for ultrasonic assisted turning. A case studies for chips produced had done and compared for with and without friction. It was found that the chip thickness ratio attained higher value and the chip radius curvature approximately four times

greater in their analysis with friction for both conventional turning and Ultrasonic assisted turning.

A study of different horn with aluminum and stainless steel as the horn material and their FEM analyses had been done by K. H. W. Seah et al. [14]. The design of stepped horn and conical horn made of both aluminium and stainless steel and was tuned to the ultrasonic machine. FEM analysis of different horn had done by carrying modal analysis and they found the frequency by simulation close to expected frequency 20 kHz. They also found that neither the addition of tool, nor the hollow tube nor the additional nodes along the length of horn causes changes in frequency. In Conical horn stresses induced was fairly low as a result it difficult to failed by fatigue or by yielding. However a high stress concentration generated at the junction of two different diameters due to sudden change in diameter that leads to failed by fatigue or by yielding. Hence it was advisable not to use stepped horn where high amplification required in Ultrasonic vibration.

N. Ahmed et al. [15] had performed 3D model and 3D effects in turning such as analyzing the chip formation, influence of tool geometry, cutting forces and stresses generated in the workpiece material. They study the effect of cutting parameters and the effect of friction on UAT and CT. For the analysis they had taken Inconel 718 workpiece material and the cutting tool taken as tungsten carbide material. They utilized MSC MARC/MENTAT FE code for FE model which is based on the updated langrangian analysis that provides transient analysis for elastoplastic materials and to analysis frictional contact between tool-workpiece contact zones. A comparison had done on 3D thermo-mechanically coupled FE approach between Ultrasonic assisted turning and conventional turning. They found that, cutting force for UAT was about 40% of that CT but experimental results showed the force in UAT was 0.25-0.6 of force in conventional turning for various feed rate. In simulation they found that for doubling the feed rate from 0.1 to 0.2 mm about 45% increasing cutting force induced because of higher material removal rate. However experimentally results showed about 50% increasing cutting force in UAT when feed rate changes from 0.05 mm/rev to 0.1 mm/rev. According to their simulation results obtained for both with and without friction corresponding to both dry and lubricating conditions showed the cutting force was about 10-15% lowered and about 30% decreased cutting force when the lubricating condition was applied. In simulation, they found that the temperature

along the cutting edge reached at a higher value in the middle because of convective heat dissipation. According to their simulation result, as the amplitude of vibration increased from 7.5  $\mu\text{m}$  to 30  $\mu\text{m}$  showed about 52% decreased in the average cutting force in UAT because of increased part of the cycle of ultrasonic vibration and also found that as frequency of vibration increasing from 10 kHz to 30 kHz induced about 47% reduced average cutting force because of the increased number of micro impacts between the tool tip and the workpiece. Hence from their analysis I found that increase in either frequency of vibration or amplitude of vibration leads to decrease in cutting force in ultrasonic assisted turning process which not only improve the accuracy of cutting process but also improve material removal rates.

A. Celaya et al. [16] had done experimental studies on mild steel workpiece material and tried to find the advantages and drawback of UAT. They had done several experiments by varying the cutting speed, feed and depth of cut in the UAT process to make the relation with the surface roughness. They proposed a booster design with varying cross-section based on the longitudinal vibration for higher amplification of vibration. They also studied the effects of the ultrasonic vibration in the two directions. Their experiments showed the improvement of surface roughness about 40% when the vibration was applied along the cutting velocity direction and about 6% improvement when the vibration was applied in the feed direction. Hence we can conclude that vibration in the cutting velocity direction reduces the waviness of geometry generation which leads to a better surface quality when compared to feed direction of vibration as well as conventional turning. According to their studied they gave two aspects. In their first aspect, the reduction of the surface roughness and the relation between the vibration and the chip removal formation does not explain completely. In their second aspect contained experimental character and it was improved reliability and the stiffness of the experimental devices. Both aspects had been found in their experiments as the joints loosening and the chatter vibrations because of the lack of stiffness were suffered. To reach a higher vibration velocity, more ultrasonic amplitude of vibration need to superimpose on the tool tip was desirable. For achieving these above criteria a new booster was proposed by them which were based on the longitudinal vibration of variable section. The main motive of the new design booster was to increase or amplify the ultrasonic vibration amplitude of the transducer generated to ensure that the sufficient vibration for machining was transmitted to the tool tip. The newly design booster material was taken AISI 1045 steel of length 150 mm having exponential profile and was found



amplification of 3:1. They found about 35% in the improvement of surface roughness by machining medium alloy steel with feed rate 0.1 mm/rev, depth of cut of 0.5 mm and cutting speed of 70 m/min.

A study on different horn shape available for ultrasonic vibration and numerical simulation using finite element had been done by M. Nad [17]. They have given some geometrical parameters of sonotrode shapes shown in Table 2.2 below

**Table 2.2** Geometrical parameters of sonotrode shapes [17]

Sonotrode Shape	Slenderness ratio	Shape parameters	Shape Function
Cylindrical	$D_0/l_0$	-	$R = D_0/2$
Tapered		$\alpha \in (-5^\circ; 5^\circ)$	$R(x) = \frac{D_0}{2} (1 + l_0 \tan(\alpha))$
Exponential		$a \in (0.3; e)$	$R(x) = \frac{D_0}{2} a^x$
Stepped		$\eta = \frac{l}{l_0}$ $\eta = \{0.25; 0.5; 0.75\}$	$R \{x \in (0; l)\} = \frac{D_0}{2}$ $R \{x \in (l; l_0)\} = \frac{D}{2}$

Where  $D_0$  is the outer diameter,  $l_0$  is the total length  $\alpha$  is the taper angle  $D$  smaller diameter in stepped horn  $l$  length of smaller diameter.

The main dynamic characteristics such as natural frequencies and amplification factors in the resonant state were analyzed for different available geometrical shapes for ultrasonic vibration was studied by them. They found that the efficiency and performance of UAT depends on the design of sonotrode and relatively large number of parameters. The selection of available sonotrode shape or horn shape depends on the technological operation to be performed on which the amplitude of vibration at the output ends to be required. They had given a conclusion that the geometrical shapes and dimensions affect the mass and stiffness distribution which affect the amplification factor of the specific horn or sonotrode. They found that for increasing cross-section and growing slenderness ratio of the sonotrode or horn leads to decreasing the amplification factor. Design of sonotrode shapes had given emphasis for ultrasonic operation in

axial direction and for radial direction sonotrode, it was necessary to ensure that it should have sufficient bending stiffness.

The roughness and roundness of the UAT where vibration given in feed direction were compared with conventional turning process by V. I. Babitsky et al. [18]. For the analysis they had taken Inconel-718, C-263 and mild steel as workpiece material. They had used different cutting condition for different material for the analysis. They found the result from their experiment that improvement of surface finish for aviation material was about 25-40% with vibration compared to conventional cutting and the improvement of roundness were achieved to 40%. For Inconel-718 workpiece material, the surface finish achieved was 40-50% and about 40-60% achieved for roundness. For the C263 workpiece material the surface finish improved were about 20-25% which was less significant than Inconel-718 and about 25-40% improvement in roundness achieved. The application of vibration in feed direction in UAT seems less limiting compared to tangential vibration. The surface finish obtained through UAT process was much superior to conventional cutting process because of reduction of low wavelength components produced.

An experimental investigation on UAT and also on mechanism of chip removal for turning NiTi based shape memory alloy along with FEM analysis of horn for finding optimum profile of horn was done by J. Akbari et al. [19]. They used Solidworks software for modeling of the horn profile and the drawing generated for manufacturing of horn. For the FEM analysis they used ANSYS software to perform modal analysis for finding nodal point for clamping. Nitonols or NiTi was high ductile, strength for creep, fractures and corrosion resistance alloy. Due to ductile behavior it can resist high strain before fracture but hardened due to strain. The problem faced by them while machining of NiTi alloy were tool wear, chip sticking, burr generation after turning. A comparison had been done by them based on roughness achieved for different cutting speeds for both UAT process and conventional process. They found better surface quality of machined surface in UAT process compared to conventional turning. They had given conclusion that about 20-70% improved surface finish achieved using ultrasonic vibration at a cutting speed range from 25-100 m/min. For mild steel workpiece about 130% improvement in surface quality at a cutting speed range from 25 to 220 m/min. Scattering of Surface roughness found to be comparatively low as compared to conventional turning.

R. Muhammad et al. [20] had done experimental investigation using a new hybrid technique called hot Ultrasonic assisted turning to machined Ti-based alloy. They combine both non-conventional techniques UAT with a traditional hot machining technique to get advantages of both combinations to machine Ti-based alloy. Ti-based alloy was experimentally and numerically analyzed over a wide range of industrially relevant speed, feed combinations for titanium alloys. Cutting condition given in Table 2.3 given below.

**Table 2.3** experimental cutting conditions [20]

Parameters	Magnitude
Cutting speed (m/min)	10
Depth up cut ( $\mu\text{m}$ )	100-500
Feed rate ( $\mu\text{m}/\text{rev}$ )	100
For HUAT maintained temperature	300
Frequency (Hz)	20
Amplitude ( $\mu\text{m}$ )	8

They had taken tool material as micro cemented carbide of (Ti,Al) N-TiN coating having  $14.6^\circ$  rake angle and of nose angle about  $55^\circ$ . They had concluded that the cutting forces significantly reduced in hot ultrasonic assisted turning. They found that with the application of external heat to the workpiece material an increase of temperature at process zone. A significant improvement of the surface roughness of machined surface found with the application external heat in both CT and UAT. They found a good agreement between simulations with the model and with the experimental data.

An experimental test investigation done for aluminium alloy Al2024 reinforced with SiC particles by using polycrystalline diamond tool to find the effect of tool geometries on the cutting force and the surface roughness by G. Dong et al. [21]. They found that the nose radius and the rake angle of tool geometry significantly influence the cutting force. A rise in cutting forces found with increasing tool nose radius, however feeding force  $F_y$  decreased with increasing of tool nose radius until the tool nose radius reached a value 0.6 mm after that it was going on increasing because of increasing tool side cutting edge angle leads to decreasing unreformed chip thickness. They found fluctuation in the surface roughness with the change in the rake angle. An increase in the rake angle reduced the cutting deformation causing effectively suppress the formation of BUE (build up edge) and burr formation leads to high quality surface finish,

however, the excessive rake angle decrease the strength of tool resulting severe tool wear and tool edge chipping. They had given conclusion that tool rake angle and tool nose radius had a significant effect on cutting force and surface finish. In their experimental investigation the surface roughness Ra less than 0.4  $\mu\text{m}$  had been achieved. It was found that tool wear reduced significantly in ultrasonic assisted turning as compared to conventional turning. The reduction in tool wear in the UAT process was found because of intermittent contact between tool and workpiece zone. In their investigation, tool topography showed the occurrence of tool wear on flank face dominant by abrasive wear and adhesive wear.

T. B. Thoe et al. [22] had done a review on ultrasonic machining. As we know hardness of tool material influence the material removal rate (MRR), tools wear rate and accuracy of the component. So they ranked the tool material on the basis of superiority as given below

Nimonic 80A > thoriated tungsten > silver steel > stainless steel > maraging steel > titanium > mild steel.

Finite element modeling was done to design axisymmetric horn shapes at a required resonant frequency and to assess the working stress to ensure safe stress limit. According to their review USM was preferable for machining low ductility and hardness above 40 HRC of the workpiece material. USM was stress and damage free process. Horn materials should have good soldering, brazing, good acoustic transmission, high fatigue resistance properties. Horn should possess corrosion resistance and should strong enough for screw attachment. Tool material should possess high wear resistance, good elastic property and should have optimum toughness and hardness values for the high working amplitude applications. The horn-tool design is an important part of ultrasonic vibration machining process to maximize the material removal. For USM generator, it should have minimum acoustic energy losses and very less heat generation and can accommodate any small errors found in the set-up and tool wear.

S. Amini et al. [23] had investigated for  $\text{Al}_2\text{O}_3$  workpiece material to analyze of the cutting forces, surface quality and tool wear with a poly crystal diamond insert tool material. The cutting forces in varying the cutting speeds and the feed rates were measured in both ultrasonic assisted turning and conventional turning. The tool wear was also compared in vibration turning with conventional turning. For the analysis they used ABAQUS software. In their FE simulation

in ABAQUS software they found that the excitation frequency obtained between 16 kHz to 25 kHz by selecting TETRA mesh type and 3D stress element type. After selecting element type modal analysis had been done. At first bending mode frequency was considered as much as 16 kHz and after 300 iterations, the best geometry found out and the resonant frequency obtained was 20106 Hz. Using Mohr surface roughness measurement system all test specimen surface roughness was measured. The bending mode vibration tool assembly vibrated in the cutting velocity direction at a constant frequency and amplitude of vibration. Reduced cutting force and an outstanding surface finish found in UAT as compared to conventional turning, but the tool wear increased in ultrasonic vibration turning condition. They got the result as cutting force induced increases as both the feed rate as well as cutting speed increases for both conventional turning process and ultrasonic vibration turning process. As the cutting speed and feed rate increased in vibration turning process, the surface roughness were also increased and it was found that there was no significant effect on the surface roughness based on cutting speed.

A clearly study of stepped horn and FEM had done by A. S. Nanu et al. [24]. They had done to adjust the frequency of the stepped horn by adjusting the lengths, diameters or any machining groove to get the desired frequency of vibration. They followed a path to achieve the required frequency given as followed.

- Frequency selection;
- Selection of proper material;
- Determination of velocity sound propagation in the selected material;
- Calculation of the theoretical dimension;
- Achievement of prototype test.

For FEM analysis they used COMSOL Multiphasic Eigen frequency module was used for modal analysis. For the analysis of horn they had used copper material and stepped horn shape. They showed the variation of resonant frequency with respect to radius given at the junction of two diameters showed in Table 2.4. From the table they got conclusion that as the radius at the junction of two diameter of horn increased from 0 mm to 3 mm, the resonant frequency go on increasing. So we found that for slightly increasing frequency can be achieved by increasing the fillet radius.

The resonant frequency slightly downwards can be possible by two methods given below

- By shortening length
- By making a groove at the center of gravity.

**Table 2.4** Fillet radius vs. resonant frequency [24]

Fillet radius R in mm	Resonant frequency in Hz	Change in frequency in percentage
0	19686	0
0.5	19642	-0.22
1	19666	-0.10
1.5	19694	0.04
2	19707	0.10
2.5	19735	0.25
3	19763	0.39

## 2.1 Summary

From the literature review, most of the paper describes that Cutting forces and surface roughness improved by using UAT process. UAT process is the chatter suppression dynamics process where as CT is the chatter generation dynamics process. The different parameters which affect the UAT process are the angles of tool, amplitude of vibration, cutting speed. UAT process finds suitable process to machine hard material like Ti based alloy, Stainless steel, Inconel 718.

# **CHAPTER 3**

- INTRODUCTION TO HORN
- PLANE WAVE EQUATION FOR HORN SHAPE
- CALCULATION OF NODAL PLANE
- FINITE ELEMENT ANALYSIS
- CONCLUSION

### **3 HORN DESIGN AND FE ANALYSIS**

---

#### **3.1 Introduction of Horn**

Ultrasonic vibratory horn is an element operating in a longitudinal mode used for efficient transfer of ultrasonic energy or vibration energy from a source element (transducer) to a second horn, coupler, tool or load. Equivalently, It is a transmission line, generally (but not always) providing a change of amplitude of vibration between the input ends and the output ends of the horn. The main purpose of the horn is to provide amplitude of vibration at its output end that is greater than that at the input end.

An ultrasonic vibratory horn is also known as acoustic horn or sonotrode or waveguide or probe or tool holder. The Horn is a metallic bar used to elevate the displacement oscillation in the form of amplitude of vibration which is provided by an ultrasonic transducer operating at an ultrasonic frequency range in between 20 kHz to 100 kHz.

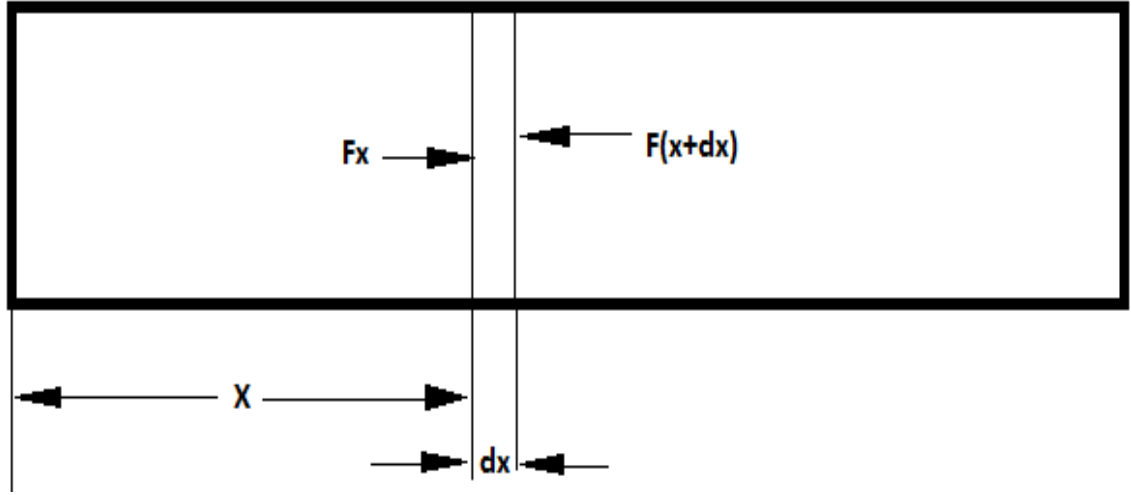
Maximum obtainable ultrasonic vibration amplitude depends not only on the properties of the material of ultrasonic horn from which an ultrasonic horn has been manufactured but also on the structural shape of the horn. Most commonly, the horns are manufactured from the material such as titanium alloys, stainless steel and aluminum alloys. The most common and simple to manufacture shapes of horn are conical and cylindrical, stepped shapes.

#### **3.2 Vibratory Tool Equation and its Solution**

##### **3.2.1 Plane wave equation**

Let's consider the motion of a plane wave propagate along X axis and the plane wave free to move in both positive and negative direction of X-axis of the slab. The respective figure shown in Figure 3.1 and respective plane wave equation explain below.





**Figure 3.1** Force propagation along the uniform slender bar

$$\xi = f_1(x - ct) + f_2(x + ct) \quad 3.1$$

Where  $f_1(x - ct)$  refers to waves moving in the positive direction of X axis of slender bar and  $f_2(x + ct)$  to waves moving in the negative direction of X axis of slender bar.  $\xi$  is the displacement of the small strip  $dx$  of the slender bar. If  $f_1(x - ct)$  and  $f_2(x + ct)$  are continuous, Equation 3.2 may be differentiated twice with respect to  $x$  (keeping  $t$  constant), given below.

$$\frac{\partial^2 \xi}{\partial x^2} = f_1''(x - ct) + f_2''(x + ct) \quad 3.2$$

Similarly equation 3.1 differentiate with respect to time  $t$  we get

$$\frac{1}{c^2} \frac{\partial^2 \xi}{\partial t^2} = f_1''(x - ct) + f_2''(x + ct) \quad 3.3$$

By comparing both equation 3.2 and 3.3 we get

$$\frac{\partial^2 \xi}{\partial t^2} = c^2 \frac{\partial^2 \xi}{\partial x^2} \quad 3.4$$

The above plane wave equation 3.4 has equation 3.1 as a general solution. Here the bar is assumed to be so slender ( $D \gg \lambda$ ) that the poisson's ratio effect is neglected where  $\lambda$

wavelength of propagated wavelength and D is the diameter of the bar. Here the sound velocity C is not defined in equation 3.4.

Let us consider a uniform, homogeneous, elastic bar having density  $\rho$ , longitudinal thickness  $dx$  and the cross sectional area  $A$  as shown figure 3.1. If we neglect the losses and by balancing forces and momentum of an element we get as shown in below.

$$F_m = Ma_c = \rho A \frac{\partial^2 \xi}{\partial x^2} dx \quad 3.5$$

Where  $M$  is the mass of the element and  $M = \rho A dx$ ,  $\xi$  is the displacement of the element  $dx$ ,  $a_c$  is the acceleration of the element is equal to  $\frac{\partial^2 \xi}{\partial x^2}$ . And  $t$  is the time against the elastic reaction of neighbored element situated between  $x$  and  $x+dx$  then equation become as given below.

$$F_{spring} = EA \frac{\partial^2 \xi}{\partial x^2} dx \quad 3.6$$

$$F_x = -EA \frac{\partial \xi}{\partial x} \text{ And } F_{x+dx} = dF_x \frac{dF_x}{dx} dx$$

From Figure 3.1,  $F_m = F_{spring}$ , so equation become

$$\rho A \frac{\partial^2 \xi}{\partial x^2} dx = EA \frac{\partial^2 \xi}{\partial x^2} dx \quad 3.7$$

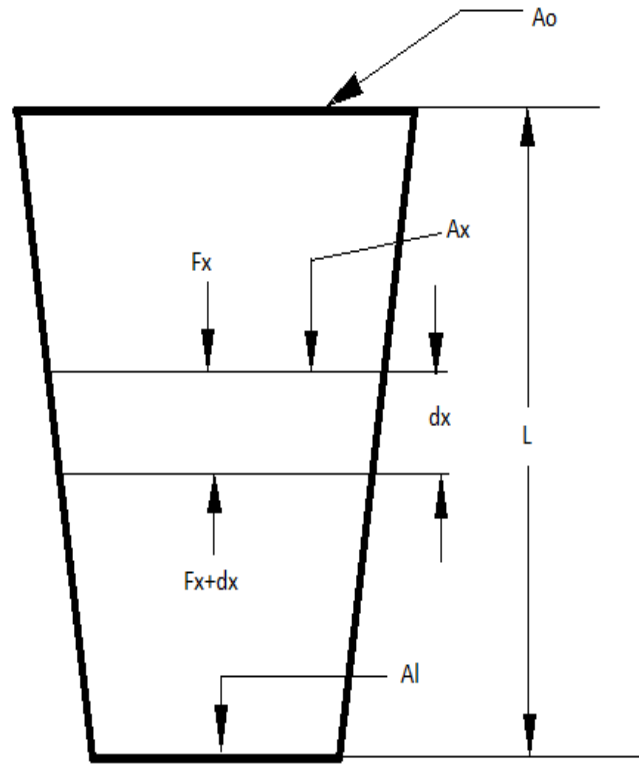
$$\frac{\partial^2 \xi}{\partial t^2} = \frac{E}{\rho} \frac{\partial^2 \xi}{\partial x^2} = c^2 \frac{\partial^2 \xi}{\partial x^2} \quad 3.8$$

$$\text{Where } C = \sqrt{\frac{E}{\rho}} \quad 3.9$$

Here  $C$  is the velocity of sound and  $E$  is the young's modulus of elasticity of the bar.

### 3.2.2 Plane wave equation of tapered horn

Let us consider tapered shaped horn shown in Figure 3.2. The wave equation for tapered horn in terms of displacement is given below.



**Figure 3.2** Propagation of wave along tapered horn shape

$$\frac{1}{c^2} \frac{\partial^2 \xi}{\partial t^2} - \frac{1}{A} \frac{\partial A}{\partial x} \frac{\partial \xi}{\partial x} - \frac{\partial^2 \xi}{\partial x^2} = 0 \quad 3.10$$

And the equation in terms of particle velocity 'v' and applying harmonic motion we get

$$\frac{\partial^2 v}{\partial x^2} = \frac{1}{A} \frac{\partial A}{\partial x} \frac{\partial v}{\partial x} - \frac{w^2}{c^2} v = 0 \quad 3.11$$

### 3.2.3 The plane wave equation for stepped type shape horn

We know that for uniform cross sectional area of a bar,  $\frac{\partial A}{\partial x} = 0$

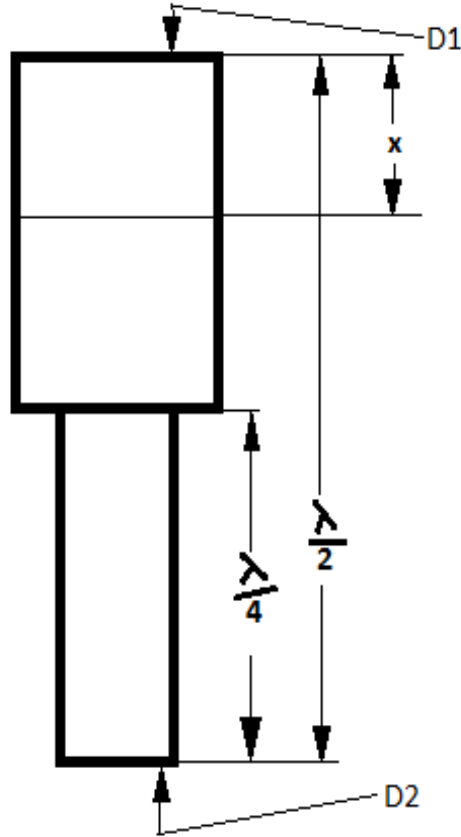
From the equation of tapered bar 3.10 and 3.11 we found that it can be reduced to a plane wave equation for which the general solution in terms of displacement  $\xi$  given as

$$\xi = \left[ A \cos \frac{wx}{c} + B \sin \frac{wx}{c} \right] \cos(wt) \quad 3.12$$

It can be written in terms of particle velocity 'v' given as

$$v = -w \left[ A \cos \frac{wx}{c} + B \sin \frac{wx}{c} \right] \sin(\omega t) \quad 3.13$$

For longitudinal half wave uniform bar shown in Figure 3.3 the equation become



**Figure 3.3** Plane wave propagated through Stepped cylindrical shape

$$\xi = \xi_M \cos \left( \frac{\omega x}{c} \right) \cos \omega t \quad 3.14$$

$$v = -\omega \xi_M \cos \left( \frac{\omega x}{c} \right) \sin \omega t \quad 3.15$$

Where  $\xi_M$  is the maximum displacement located at  $x = 0$  and the acceleration at any point  $x$  from top end along the horn is given as

$$a = -\omega^2 \xi_M \cos \left( \frac{\omega x}{c} \right) \cos \omega t \cong \omega^2 \xi \quad 3.16$$

Where  $\omega$  is the angular velocity and Stress  $S$  at distance  $x$  from top end represent as

$$S = \frac{iE}{\omega} \frac{dv}{dx} \quad 3.17$$

Where  $\omega \xi_M$  is the maximum velocity occurs at  $x = 0$ ,  $E$  is the young's modulus of elasticity and  $i$  is the complex number and the value is  $i = \sqrt{-1}$ .

For the stepped vibratory tool the step occurs at the mid plane along the length, the momentum of the elements on either side given as

$$\frac{\xi_1}{\xi_2} = \frac{v_1}{v_2} = \frac{A_2}{A_1} \quad 3.18$$

Where  $\xi_1$  and  $\xi_2$  tool is the displacement,  $v_1$  and  $v_2$  is the particle velocity and are the area of cross section at  $x = 0$  and  $x = L$ .

### 3.2.4 Calculation of nodal plane in stepped cylindrical shape horn

It is important to locate the nodal plane to clamp the ultrasonic system. Nodal plane is the plane where particle displacement of vibratory tool is zero. For the system to make rigid it is advisable to clamp the system at nodal plane. If the system clamp other than nodal plane affect the whole system by fluctuating frequency and amplitude of vibration which further affect the ultrasonic turning process.

From equation 3.14 at nodal plane  $\xi = 0$  represented as






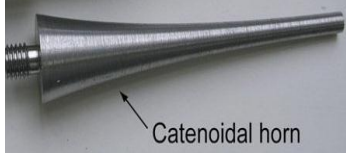
$$\cos \frac{\omega x}{c} = 0 \quad 3.19$$

$$x_n = \frac{nc}{4f} \quad 3.20$$

Where  $x$  is the nodal plane position,  $f$  is the frequency of vibration and  $C$  is the sound velocity.

Table 3.1 showing the different length and magnification factor for different horn shape collected. Horn length depends on the type of shape it possess and type of material. These parameter are collected from literature review and book.

**Table 3.1** Different Horn shape length and magnification factor

HORN TYPE	HORN	LENGTH	MAGNIFICATION FACTOR
CYLINDRICAL		$L = \frac{c}{2f}$ C-sound velocity f -frequency L=half wave length= $\lambda/2$	M=1
STEPPED HORN		$L = \frac{c}{2f}$	$M = \left(\frac{D_1}{D_2}\right)^2$
EXPONENTIAL		$L = \frac{c}{f} \sqrt{1 + (\ln N / 2\pi)^2}$ Where N-dia ratio	M=D <sub>o</sub> /D <sub>i</sub>
WEDGED SHAPED		$L = 3.2c/w$ W=2f Profile equation $S = s_1 + (s_2 - s_1)/l$	M=1.832(max)
CONICAL HORN		$L = 1.1(L_{\text{exponential}})$ Or $l = 4.5c/w$	M=4.61(max)
CATENOIDAL HORN		$L = \frac{c}{w} \sqrt{\pi^2 + \cosh^{-1} \left( \frac{kD_2}{D_1} \right)^2}$	

### 3.3 Finite Element Modeling of Ultrasonic Vibratory tool

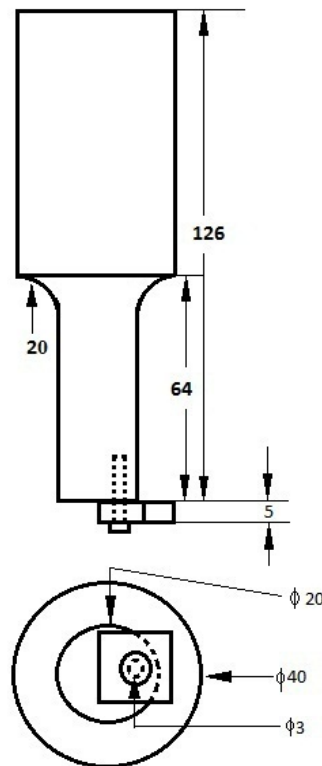
#### 3.3.1 The finite element

The finite element is the software based analysis of newly design part or product having specific material to know the stress generation for specific requirement. FEM analysis able to verify the proposed design will be able to perform or to withstand to the client's specifications prior to manufacturing or construction. In case of any failure FEM used to determine the design modification to meet the result.

#### 3.3.2 Finite element modeling of horn-tool assembly

FEM has been used for various analyses vastly. In my research ANSYS® software has been used widely for dynamic analysis of ultrasonic vibratory tool to know the frequency and amplitude of vibration and the stress generation. In this analysis modal analysis and harmonic analysis has done to calculate the natural frequency and amplitude of vibration of specific shape having specific horn material.

##### 3.3.2.1 Geometrical modeling of horn-tool assembly



**Figure 3. 4** Stepped horn specification in mm based on 3<sup>rd</sup> angle of projection

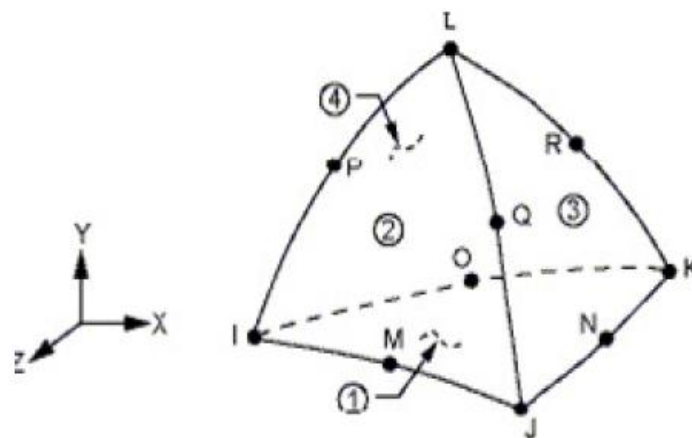
For the analysis and manufacturing stepped horn is selected because of its maximum output amplitude amplification. The total horn, tool connected with screw has been analysed to know the whole dynamic behavior. The model was difficult to do in ANSYS® APDL. So the model has done individually in SOLID WORKS software and got assembly to make the whole set whose drawing is shown in Figure 3.4 and model diagram is shown in Figure 3.5.

### 3.3.2.2 *Material property of horn-tool assembly*

For the stepped horn and screw, ‘mild steel’ is used for the analysis with material properties as young’s modulus  $E = 210 \text{ GPa}$ , density  $\rho = 7861 \text{ Kg/m}^3$  and Poisson ratio  $\gamma = 0.3$ . The theoretical frequency 20 KHz I got from 129 mm horn length. For the tool material ‘carbide insert’ is used having young’s modulus  $E = 550 \text{ GPa}$ , density  $\rho = 15800 \text{ Kg/m}^3$  and Poisson ratio  $\gamma = 0.24$ . By using equation 3.9, the theoretical length I have found 129 mm.

### 3.3.2.3 *Element type selection for horn-tool assembly*

In the analysis ‘element type selection’ is the very first process. Based on the type of analysis either 2D or 3D, input we are giving and what output we want element type selection is given. For the UAT horn analysis ‘structural analysis’ has been chosen for which ‘solid 92 and tetrahedron with 10 nodes’ selected as the type of element shown in Figure 3.5. Tetrahedron element is suitable for our analysis because it allows the finite element analysis software to grid the complex 3D geometry model easily.

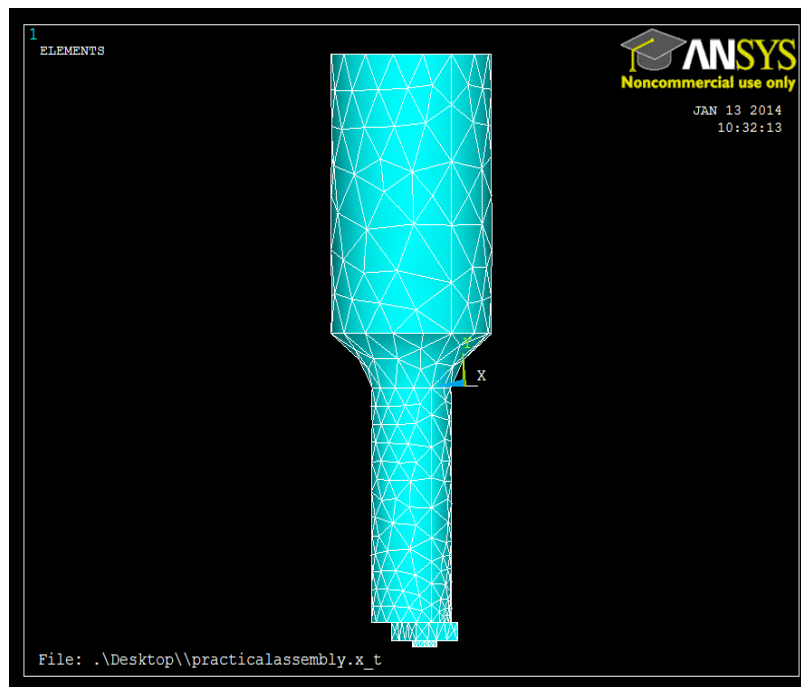


**Figure 3.5** Solid 92 elements represented from ANSYS user guide



#### 3.3.2.4 Mesh generation of horn-tool assembly

After choosing element type selection, meshing has been done for the total assembly. Mesh generation plays an important role in the analysis to get the accurate result from the analysis. If the mesh size is infinitely small, than it takes more computational time because it generate too many elements and nodes to reach optimal solution which leads to consume time to solve but it can give better output result. If the mesh size is comparatively small, than it approaches the optimum solution and less time consumption that leads to give inaccuracy output result. So it is convenient to use a reasonable mesh size for the finite element analysis. In my analysis for medium mesh 14075 nodes and 6834 elements created which is shown in Figure 3.6 given below.



**Figure 3.6** Mesh generation of horn assembly

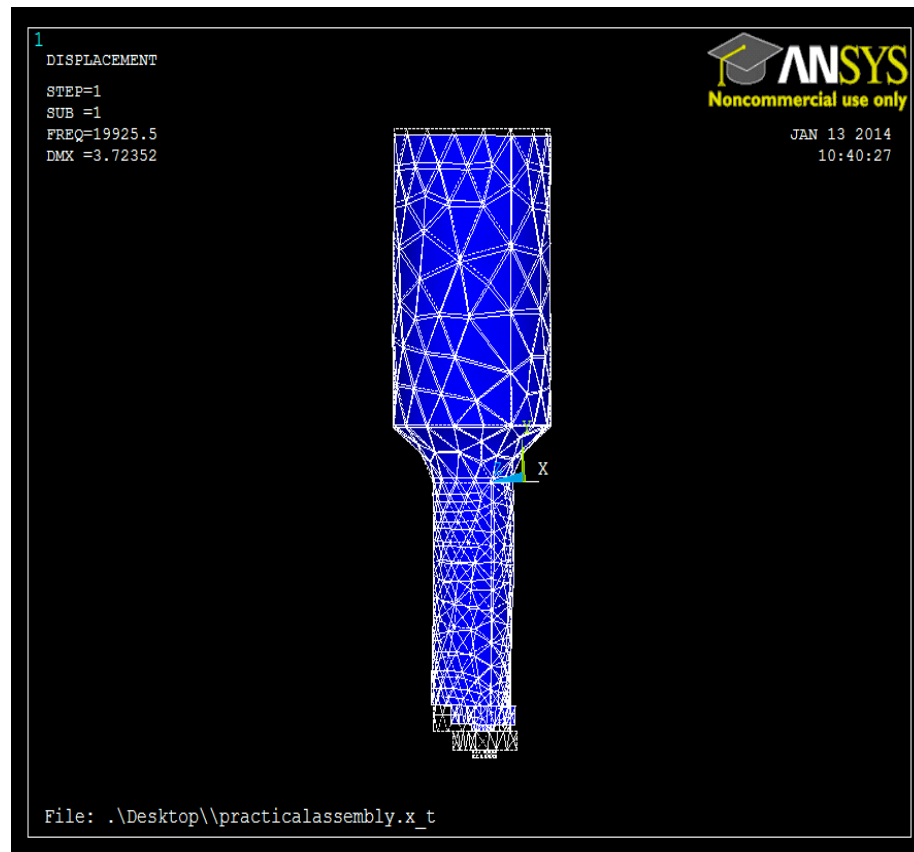
#### 3.3.2.5 Boundary condition for horn

After the mesh generation boundary condition is given for the analysis. Since the horn is connected to the output end of the transducer which generate the amplitude of vibration and transfer the vibration in terms of displacement, So boundary condition is given to the input end of horn assembly as the displacement of output of transducer.

### 3.4 Result and Analysis of Horn

#### 3.4.1 Modal analysis

Modal analysis is a linear analysis which ignores plasticity and contact element used for dynamic analysis of a specific part. Since Horn is a vibration amplifier which vibrated at a specific frequency and amplitude dynamically, so it needs modal analysis to carry out for calculate the resonant vibration and to determine the response of the horn to any type of dynamic load.

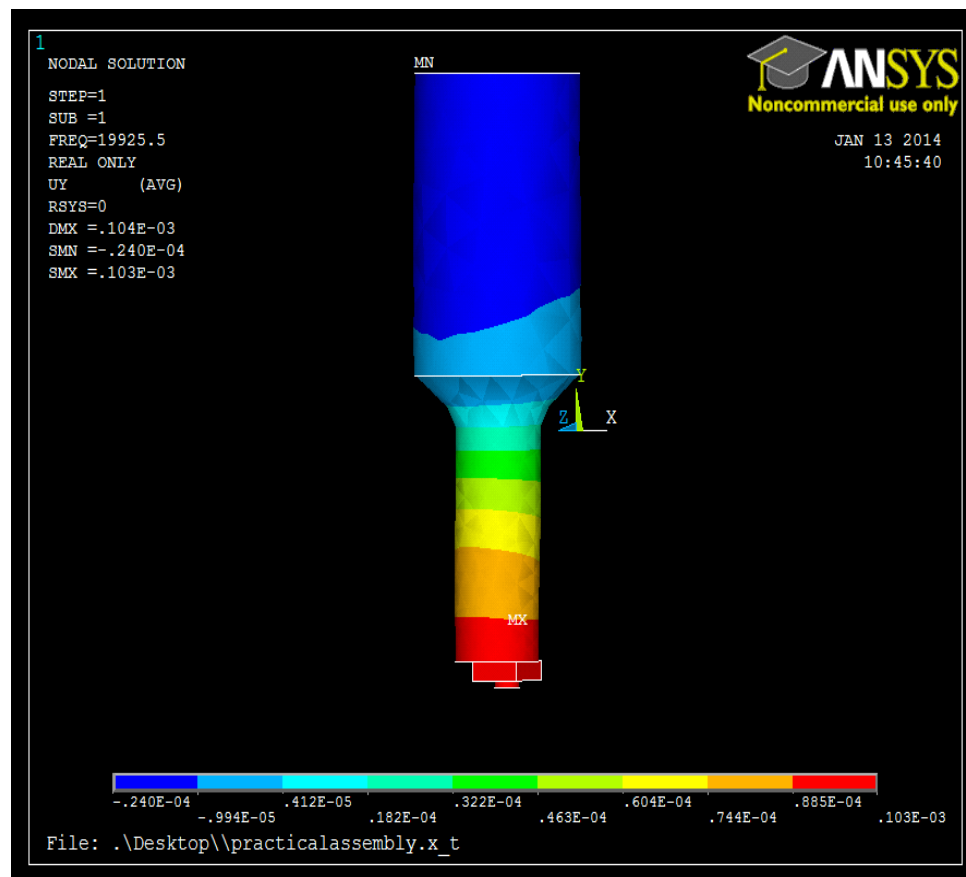


**Figure 3.7** Modal analysis results

In the Modal analysis BLOCK LANCZOS method has been used for solving the model. Modal analysis is carried out first for any analysis and the output of the modal analysis is used for other analysis. Here the output of Modal analysis is used for the input of Harmonic analysis. The output of the modal analysis is shown in Figure 3.7. We can see from the figure that it is vibrating at a natural frequency of 19925.5 Hz and how it's behave under dynamic load under vibration.

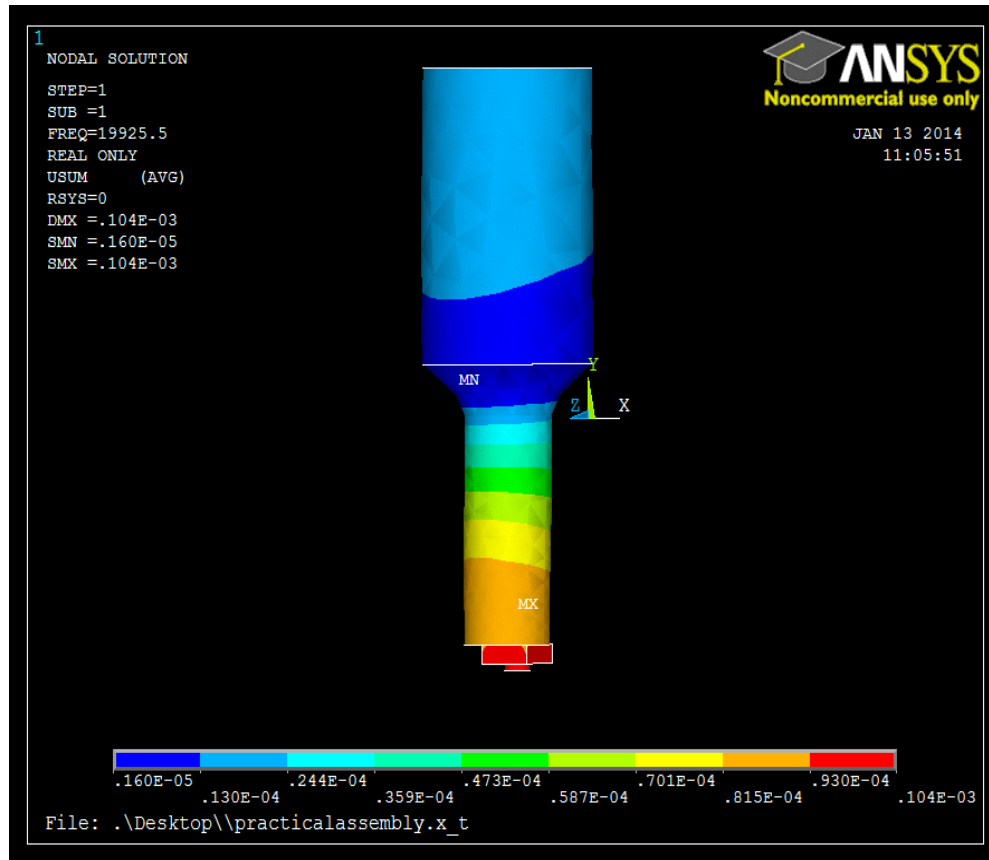
### 3.4.2 Harmonic analysis

Harmonic analysis is done by specifying the various input harmonic load such as forces, pressure and displacement of known frequency of the structure which is required for to know the response of the structure with respect to sinusoidal loads. Harmonic analysis gives the output results as stresses, strain and displacement at each DOF of the structure or the Horn assembly.



**Figure 3.8** Maximum displacement of horn assembly

The output result of harmonic analysis shown in Figure 3.8, 3.9, 3.10, 3.11. From Figure 3.9 it is clear that the initial displacement approaches to zero and the displacement is zero at the fillet area of the horn assembly. Finally the displacement increased and amplified at the end likewise Figure 3.12 has been shown.



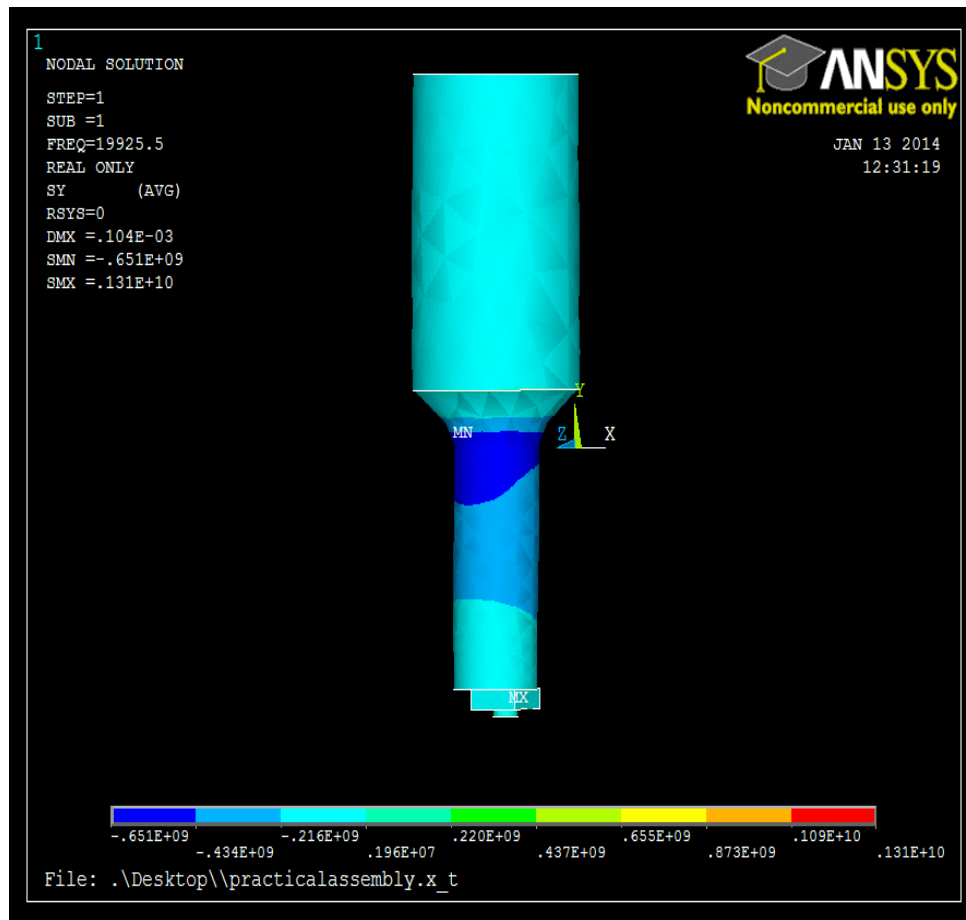
**Figure 3.9** Displacement vector sum of horn assembly

### 3.4.3 Results of FE for horn assembly

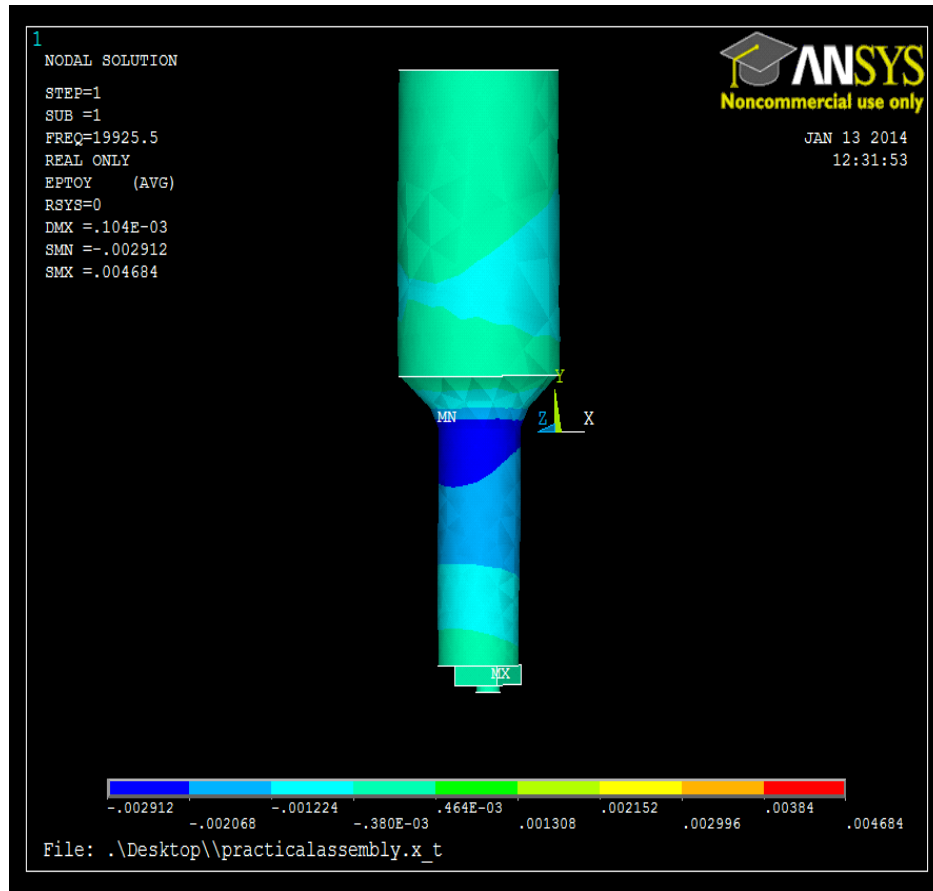
From modal analysis the stepped horn having larger diameter or input end of stepped horn 40 mm, smaller diameter or output end of stepped horn 20 mm and total horn length is about 126 mm and tool thickness is about 5 mm, I have found 19925.5 Hz frequency (Figure 3.7) at only one node which is desirable because it is close 20000 Hz which is available in the working frequency range of the generator. The length of horn is approximately close to theoretical length (129 mm from theoretical calculation).

From Harmonic analysis I found the amplitude of vibration has been amplified approximately 4 times of input amplitude of vibration (Figure 3.8 shows input displacement 24 micron and output displacement 104 micron) which means the analysis is correct and it satisfy the theoretical concept of stepped horn which is noted at Table 3.1. From the harmonic analysis a less stress has been generated at the junction of larger and smaller diameter of stepped horn which is quite natural because of zero displacement generated in the junction area of stepped

horn shown in Figure 3.10. From figure I found that minimum stress generated is -651 MPa and Maximum stress is 220 MPa.



**Figure 3.10** Stress variation of horn assembly

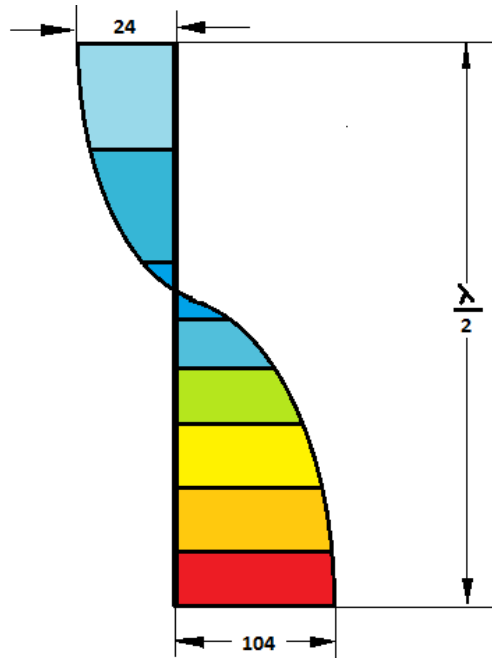


**Figure 3.11** Strain distributions

### 3.5 Conclusion

ANSYS<sup>®</sup> software is used for finite element analysis which allows modeling and analysis for testing of different ultrasonic vibrating horn shapes which helps without use of manufacture real prototype. It also helps to select the correct horn shape which vibrates at particular frequency (20 KHz) for specific operation. It also make easy to know the amplitude, stress at every point of the stepped horn which helps for improving the horn life.

It is important to get one natural frequency within the allowable frequency range and by taking mild steel material of horn and carbide insert tool material of stepped horn assembly having 131 mm length I found one natural frequency 19925.5 Hz in the frequency range of 19500 to 20500 Hz and amplitude of vibration 4 times of input vibration at output end which is shown in Figure 3.7, 3.8, 3.9, 3.10. To ensure the point of maximum amplitude or the antinode coincide with the output position of the tool, it is important that the length of horn should be half of a wavelength as shown in Figure 3.12.



**Figure 3.12** Wave propagates in micron amplitude through horn assembly

From the results, it can be conclude that the analysis of stepped horn by taking mild steel horn material, carbide as tool material is correct and it also satisfy theoretical concepts of horn shape.

# **CHAPTER 4**

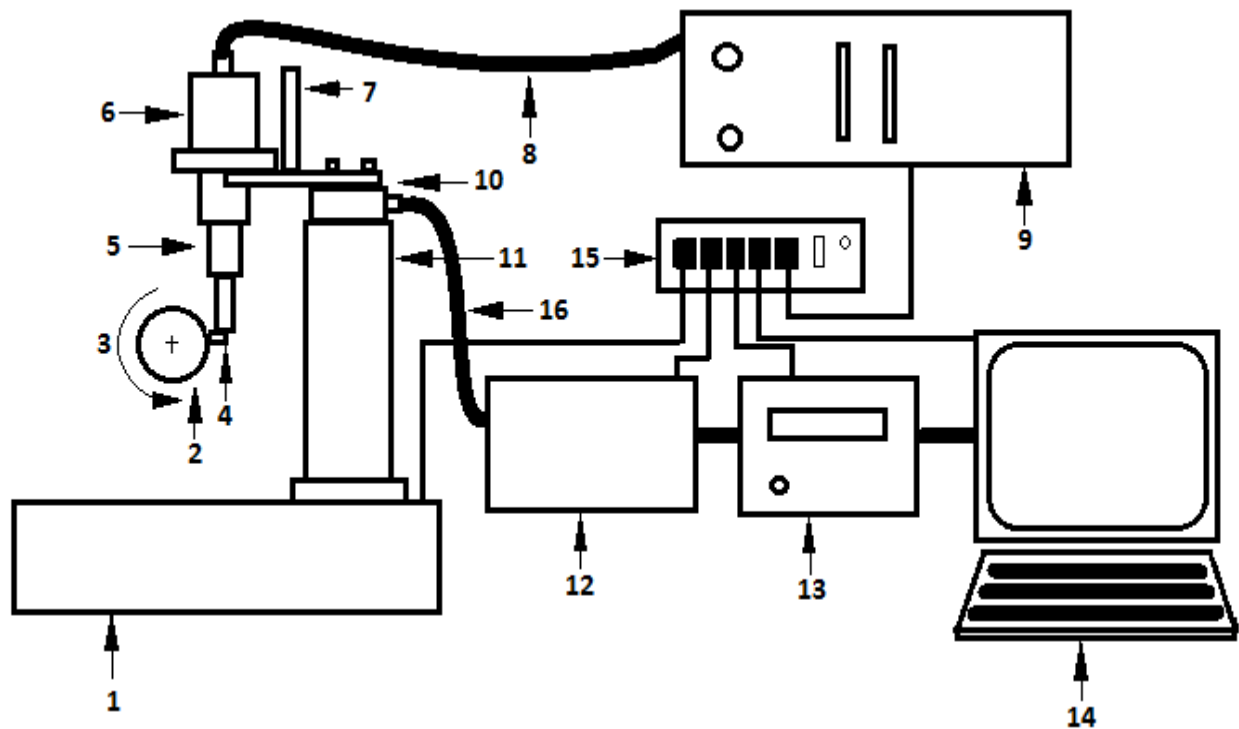
- **EXPERIMENTAL SETUP**
- **EXPERIMENTAL CONDITION**
- **RESULT AND DISCUSION**
- **CONCLUSION**



## 4 EXPERIMENTAL INVESTIGATION

### 4.1 Experimental Set-up and Description

The experimental set-up is the arrangement of different parts which is relevant to the experiment and connected sequentially to get the better result. The set-up should be error less and rigid enough to withstand vibration. The ray diagram is shown below in Figure 4.1 and the set-up is shown in Figure 4.4.



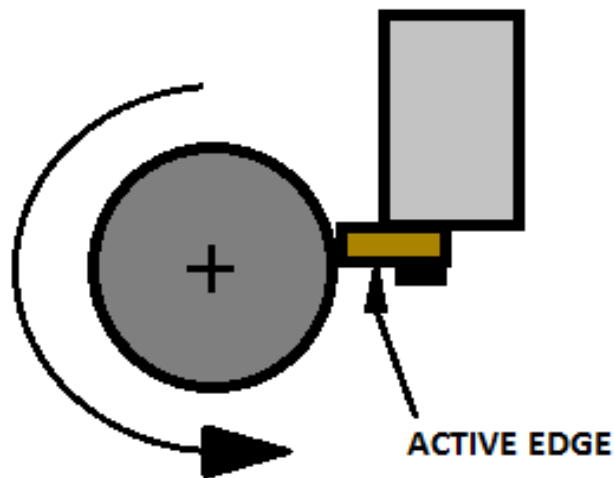
**Figure 4.1** Semantic diagram of Experimental set-up of UAT

1. HMT NH-26 lathe
2. Workpiece rotate anti-clockwise
3. Anti-clockwise rotation of workpiece
4. Carbide insert tool connected to stepped horn by screw
5. Stepped horn connected to transducer
6. Transducer
7. L-shape bracket for holding transducer
8. HF (high frequency) cable

9. Ultrasonic generator
10. Dynamometer (Kistler model 9272)
11. Height adjustable cylindrical column
12. Charge amplifier model 5070A
13. Data acquisition system
14. PC (control system)
15. Power supply
16. Dynamometer cable

#### 4.1.1 Description of the machining process

The semantic diagram of the set-up is shown in Figure 4.1 and the parts are described under the diagram. The workpiece is rotated anticlockwise by HMT NH 26 lathe machine as the tool bottom part is the active cutting edge as shown in Figure 4.2 which is zoom part of machine zone. The horn attached with tool by screw bolt which is further attached with pizo-electric transducer where the vibration generated in the form of ultrasonic sound which is powered by Ultrasonic generator by HF (high frequency) cable. Ultrasonic generator supplies the high frequency in the range of  $20 \pm 0.5$  KHz which required 230 V, AC current supply.



**Figure 4.2** Rotation of work piece with respect to active edge of cutting tool

At the nodal point of the ultrasonic transducer clamped by L shaped bracket (Figure 4.1) which is further connected above the Kistler dynamometer by number of screw bolt. The dynamometer is used to measure the forces induced in machining process and is generated digital

signal. The dynamometer is placed above the height bar by screw bolt and the height bar consist of no of bars connected by Allen bolt and is selected with respect to the height to be maintained or the tool tip should be in center line position. The base of height bar placed above the carriage of the HMT NH 26 lathe. The dynamometer send the digital signal to charge amplifier and further goes to data acquisition system and the digital signal stored in every mili sec which helps to plot the graphs through we can know how the forces varies for a particular machining process.

The following tables are the specification of ultrasonic generator (Table 4.1), Kistler dynamometer (Table 4.2).

**Table 4.1** Specification of ultrasonic generator

Voltage	230 V
Current	6 A
Input frequency	50 Hz
Output frequency	20,000 Hz
Power output	2 KW
Amplitude	24 $\mu$ m
Operation mode	Pulse mode and continuous mode
Mode of tuning	Auto/Manual

**Table 4.2** Specification of Kistler Dynamometer 9272

Measuring parameter	In the limit of
Cutting force	-5 to 5 KN
Feed force	-5 to 5 KN
Radial force	-5 to 5 KN
moment	-0.2 to 0.2 KN-m

Specification of control unit PC should have 526 MB RAM, Pentium 4 processor and 800\*600 resolutions and should have window XP operating system. For Data acquisition system should have USB based fourteen bit and eight channel data card.

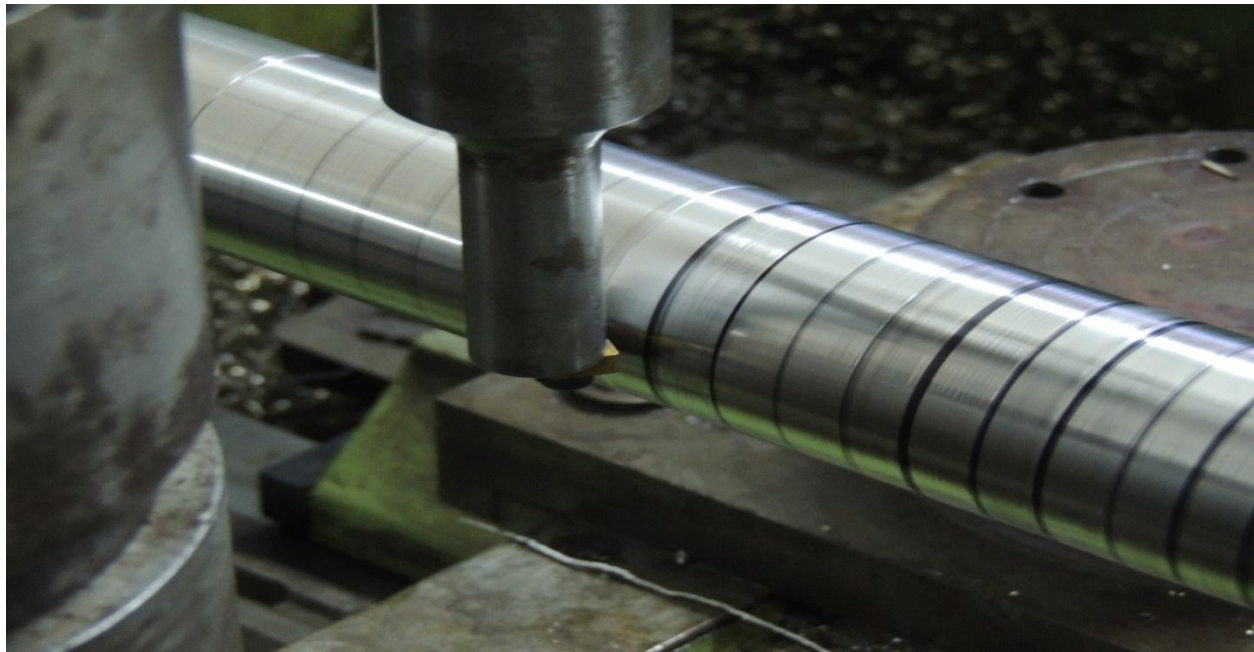
#### **4.1.2 Work piece processing**

Stainless steel cylindrical work piece having 50 mm diameter is chosen for the experimental cutting process. First 12 mm length cut in conventional turning process after that ultrasonic vibration given to the tool for another 12 mm of length. This process is continuing for each run. For each run the machined surface having two surfaces generation namely first

conventional machined surface and ultrasonic vibration machines surface and will be marked for measuring surface roughness as shown in Figure 4.4.



**Figure 4. 3** Experimental set-up (a) UAT base, (b) DAQ system connected to amplifier with PC



**Figure 4.4** CT and UAT machined work piece

#### 4.1.3 Cutting force measurement

The induced force generated from machining zone transfer through tool, horn, transducer and L-shaped bracket onto the dynamometer as shown in Figure 4.1. As we know that dynamometer generate digital signal transfer into charge amplifier which having small display for forces and further data transferred onto Data acquisition system and connected to PC to store the forces with respect to time (sec). In Data acquisition system channels has to set and it will show three forces which will be display through PC. Finally the induced force will be stored and the graph with respect to time will be generated with the use of software on computer as shown in Figure 4.1.

#### 4.1.4 Surface roughness measurement

After finishing each run, the surface generated by ultrasonic vibration turning process and conventional turning process the surface roughness has been measured. HANDYSURF precision instrument has been used for measuring surface roughness of each run of the experiment. Through HANDYSURF center line average roughness denoted as  $R_a$  has been noted for each run for both ultrasonic assisted turning and conventional turning process and has been analyzed to get the interaction relation between different process parameters ( cutting velocity, feed rate, depth of cut ).

### 4.2 Experimental Condition

Three factor namely cutting velocity, feed and depth of cut and each having three level chosen for the experimentation. Total 9 runs have been done for both CT (conventional turning) and UAT (ultrasonic assisted turning) process. Table 4.3 describes the cutting condition.

**Table 4.3** Cutting condition for experimentation

Material of work piece	Cutting velocity ' $V_c$ ' m/min	Feed ' $f$ ' in mm/rev	Depth of cut ' $d$ ' in mm
Stainless steel	22.77	0.06	0.15
	38.48	0.07	0.2
	65.97	0.08	0.25

### 4.3 Experimental Results and Discussion

After experimentation results stored in DAQ extracted and plot the graphs needed and the average Cutting force, Thrust force and feed force noted down. After the experiment over,

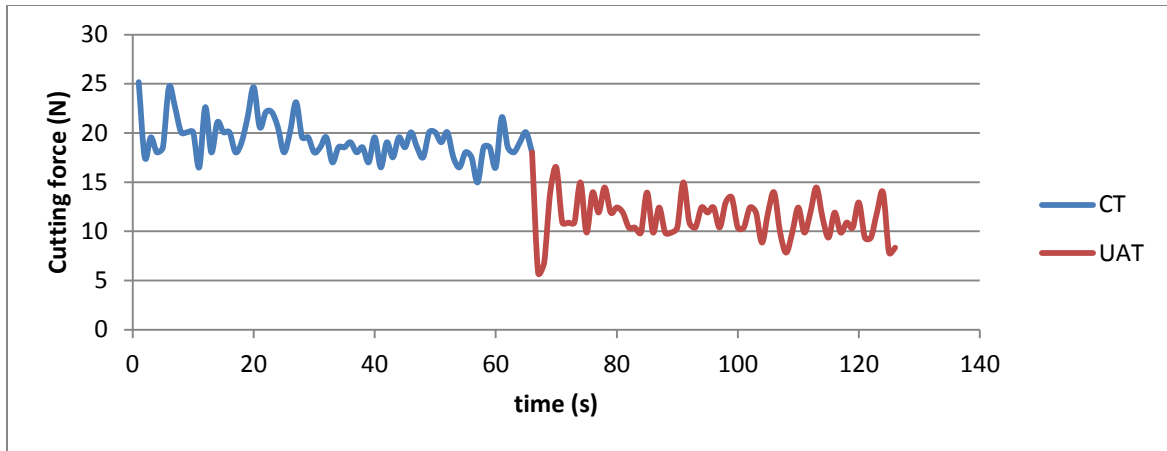
surface roughness Ra measured by HANDYSURF for each run and noted down. Table 4.4 showing the results obtained from experiment.

**Table 4.4** Experimental results obtained

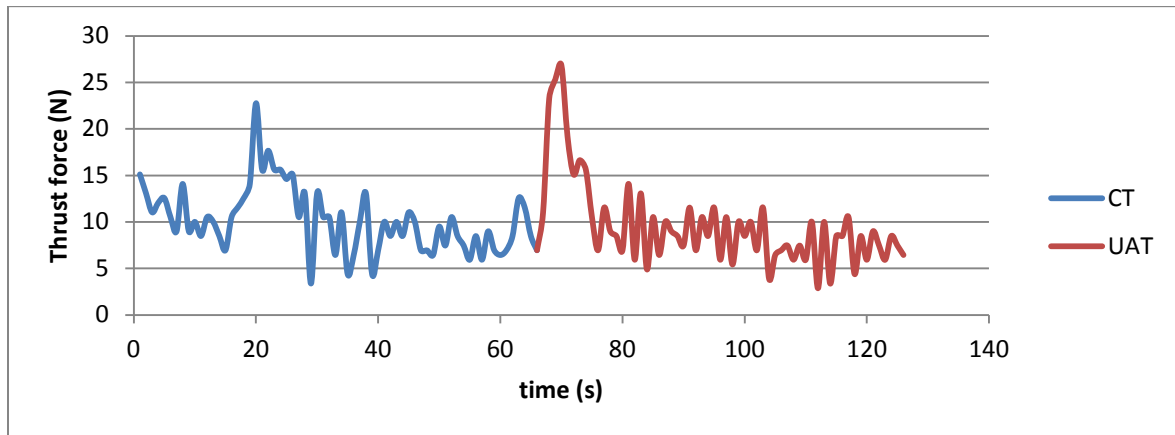
Process Parameter			Conventional Turning				Ultrasonic Assisted Turning			
$V_c$ In m/min	$f$ in rev/min	$d$ in mm	Cutting force in N	Thrust force in N	Feed force in N	Surface roughness Ra in $\mu\text{m}$	Cutting force in N	Thrust force in N	Feed force in N	Surface roughness Ra in $\mu\text{m}$
22.77	0.06	0.15	19.336	10.149	2.982	1.2	11.289	9.593	1.37	0.8
22.77	0.07	0.2	30.085	69.119	30.2	1.6	24.688	65.77	29.9	0.9
22.77	0.08	0.25	36.477	75.37	29.9	1.2	23.549	67.36	27.3	0.8
38.48	0.06	0.2	25.763	44.661	12	0.7	11.878	25.87	2.55	0.4
38.48	0.07	0.25	41.682	79.21	24	0.9	29.399	67.64	23.5	0.5
38.48	0.08	0.15	42.995	112.22	49.3	0.8	38.326	111.5	47.6	0.7
65.97	0.06	0.25	30.067	60.096	18.89	0.7	24.014	60.55	19.1	0.6
65.97	0.07	0.15	59.83	154.37	48.37	0.7	54.942	163	47.4	0.5
68.97	0.08	0.2	65.644	180.69	39.82	0.7	57.767	173.2	41.3	0.6

Figure 4.5 obtained for the first run having 22.77 m/min, 0.06 mm/rev of feed and depth of cut 0.15 mm. From figure CT and UAT forces induced is noted by blue and red line. From the figure it is clear that when ultrasonic vibration given to the tool, the cutting force suddenly drop to some extent after it is constantly linearly vary with respect to time. The average cutting force induced in CT is 19.36 N and for UAT 11.289 N. So difference is clearly visible. Thrust force is almost constant for both CT and UAT. So we can tell in low speed, low feed and low depth of cut ultrasonic vibration has less effect in thrust force. Feed force also affected a little due to ultrasonic vibration machining. So UAT reduces all the forces to some extent as shown in Figure 4.5.

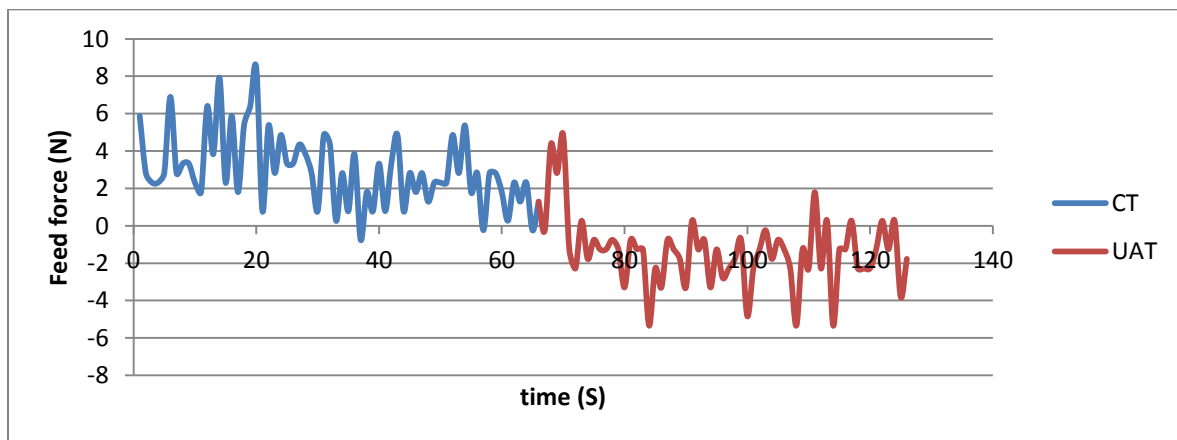
The graphs have been plotted for 2<sup>nd</sup> run having 22.77 m/min, 0.07 mm/rev of feed and depth of cut 0.2 mm has been shown in Figure 4.6.



(a)

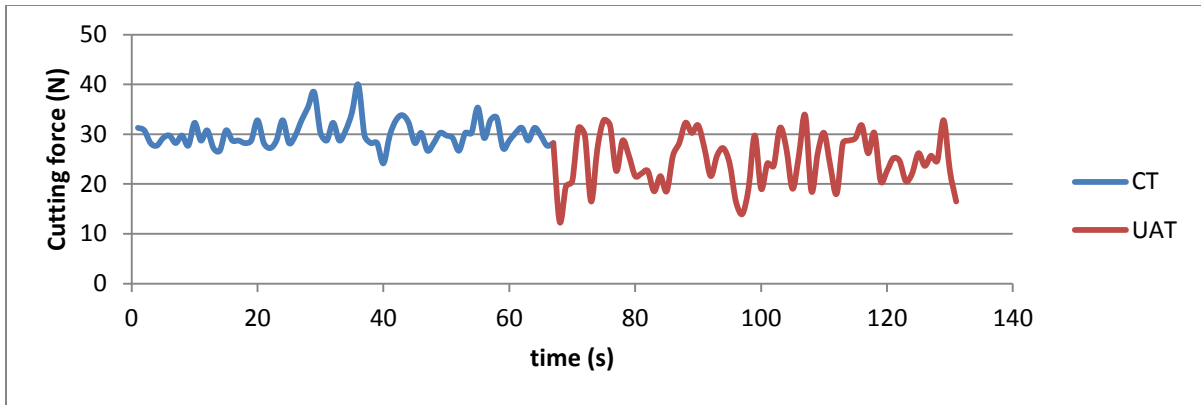


(b)

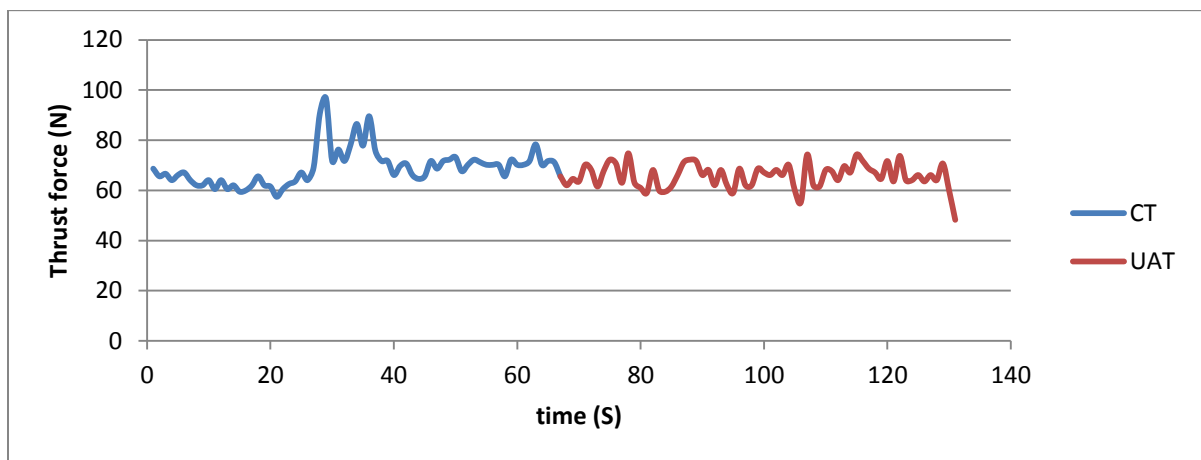


(c)

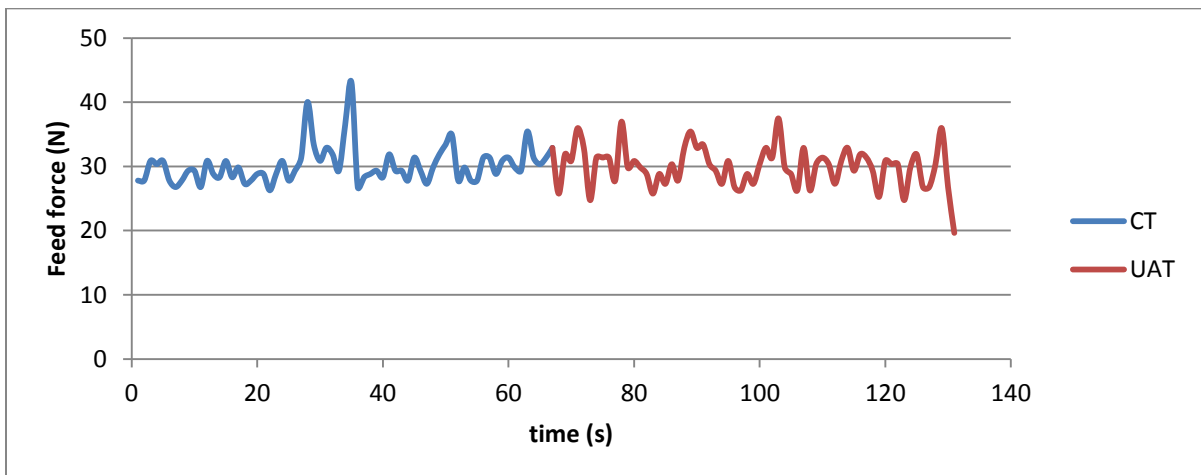
**Figure 4.5** Graph plotted between (a) cutting force vs. time, (b) Thrust force vs. time, (c) Feed force vs. time for 1<sup>st</sup> run defined in Table 4.4



(a)



(b)



(c)

**Figure 4.6** Graph plotted between (a) cutting forces vs. time, (b) Thrust force vs. time, (c) Feed force vs. time for 2<sup>nd</sup> run defined in Table 4.4



From the Figure 4.6, we can observed that, at first forces induced in CT noted in blue color after 65 sec Ultrasonic vibration is given, hence the difference is Cleary observed by red color. The average cutting force induced for CT is 30.085 N and for UAT 24.688 N has been obtained. So difference is clearly visible. So average cutting force induced in UAT is reduced as compared to CT. Feed force and Thrust force is almost constant for both CT and UAT.

For 3<sup>rd</sup> run having cutting velocity 22.77 m/min, 0.08 mm/rev and depth of cut 0.25 has been shown in Figure 4.7. Average cutting force induced in CT is 36.477 N and for UAT 23.549 N. So difference is clearly observed in the Figure 4.7. Feed force and Thrust force is approximately constant for both CT and UAT process.

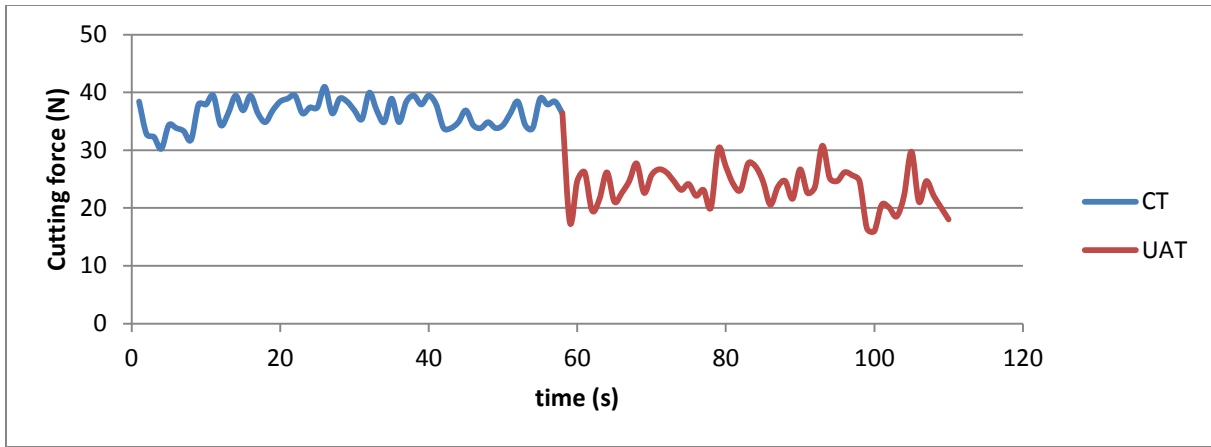
For 4<sup>th</sup> run having 38.48 m/min cutting velocity, feed 0.06 mm/rev and depth of cut 0.2 mm has been shown in Figure 4.8. The average cutting force induced in CT is 25.763 N and for UAT 11.878 N. So difference is clearly visible by the blue color (CT) and red color (UAT). Thrust force and feed force has been also affected by ultrasonic vibration as a result it also reduce a little bit as shown in Figure 4.8.

For 5<sup>th</sup> run having 38.48 m/min cutting velocity, feed 0.07 mm/rev and depth of cut 0.25 mm has been shown in Figure 4.9. The average cutting force induced in CT is 41.682 N and in UAT 29.399 N. So it reduced the cutting force about 29.46%. In the graph the difference is clearly visible. Thrust force and feed force are approximately constant for both CT and UAT as shown in Figure 4.9.

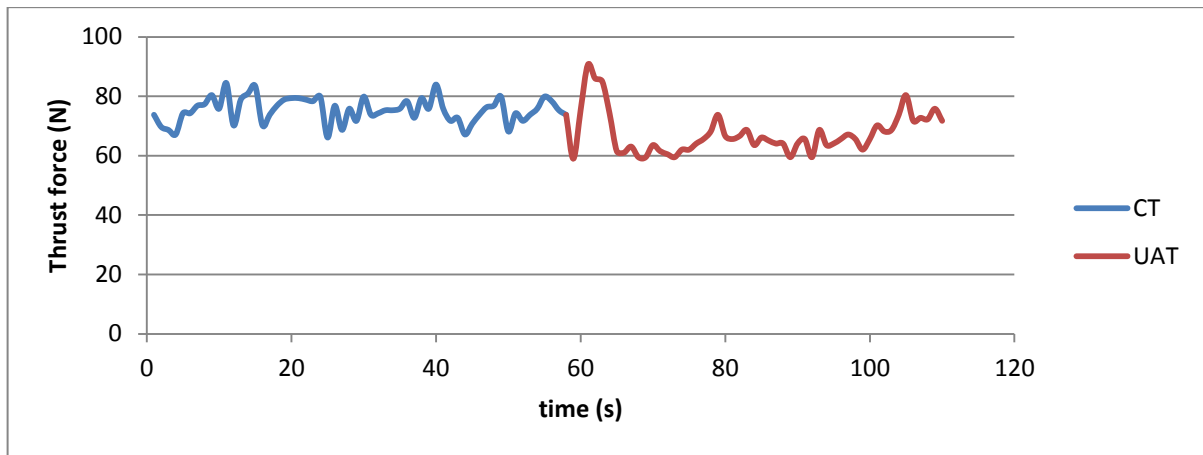
For 6<sup>th</sup> run having 38.48 m/min cutting velocity, feed 0.08 mm/rev and depth of cut 0.15 mm has been shown in Figure 4.10. Here also we can observe the same pattern as earlier. Feed force and Thrust force are less affected by ultrasonic vibration cutting.

For 7<sup>th</sup> run having 65.97 m/min cutting velocity, feed 0.06 mm/rev and depth of cut 0.25 mm has been plotted in Figure 4.11. Here also we observed the same pattern discussed above.

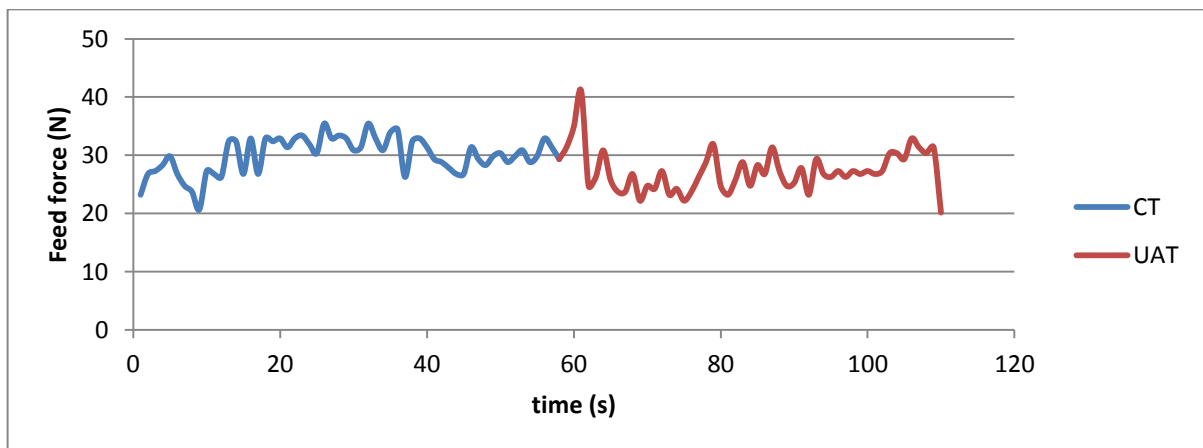
Similarly for 8<sup>th</sup> and 9<sup>th</sup> run graphs has been plotted in Figure 4.12 and 4.13. Here also we can observe the cutting force reduces a little bit compared to CT. Thrust force and feed force also approximately constant.



(a)

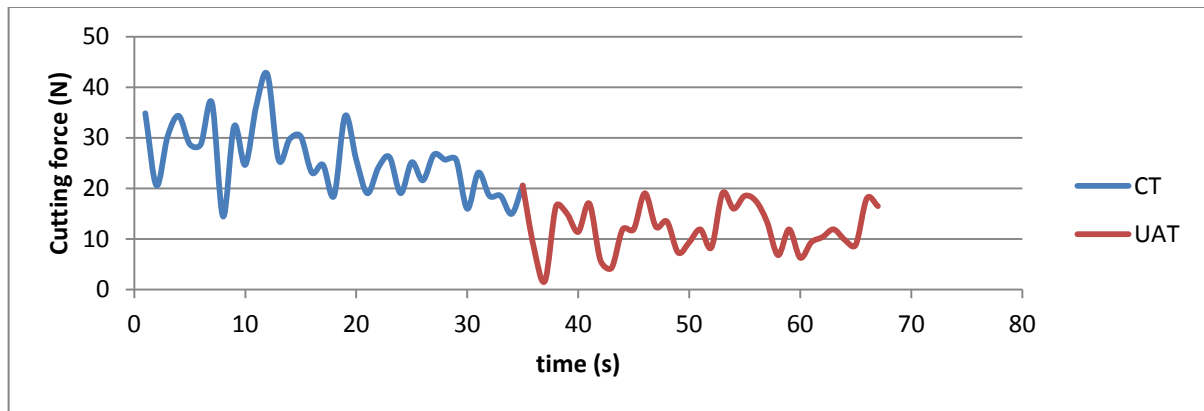


(b)

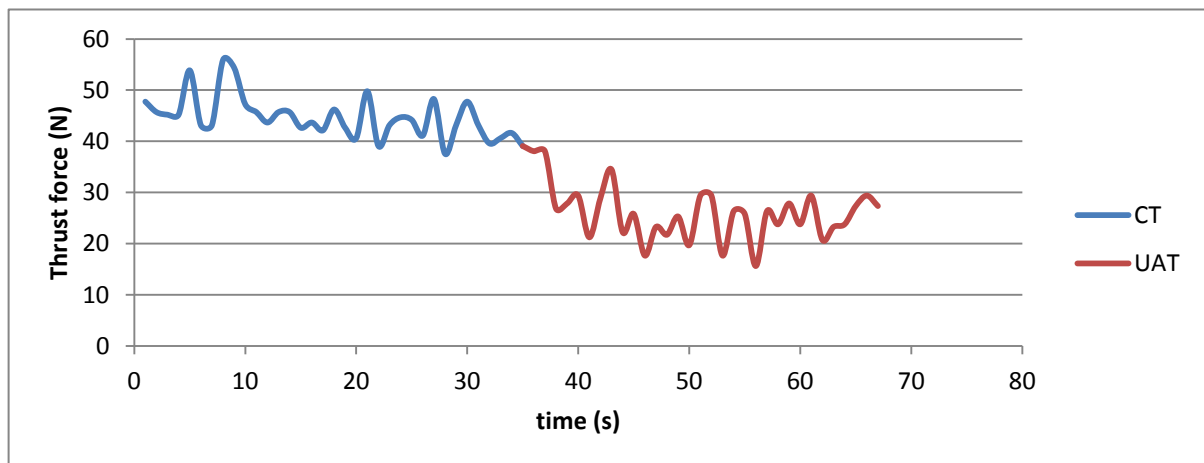


(c)

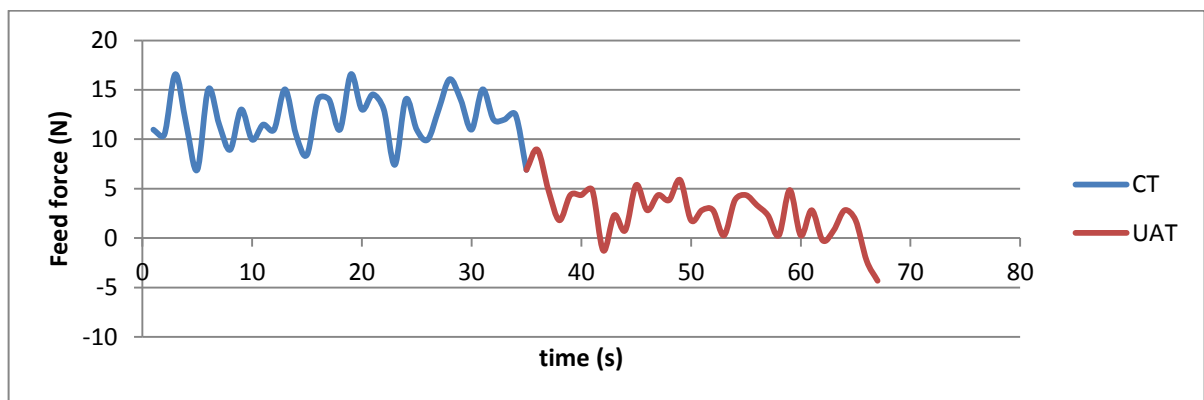
**Figure 4.7** Graph plotted between (a) cutting forces vs. time, (b) Thrust force vs. time, (c) Feed force vs. time for 3<sup>rd</sup> run defined in Table 4.4



(a)

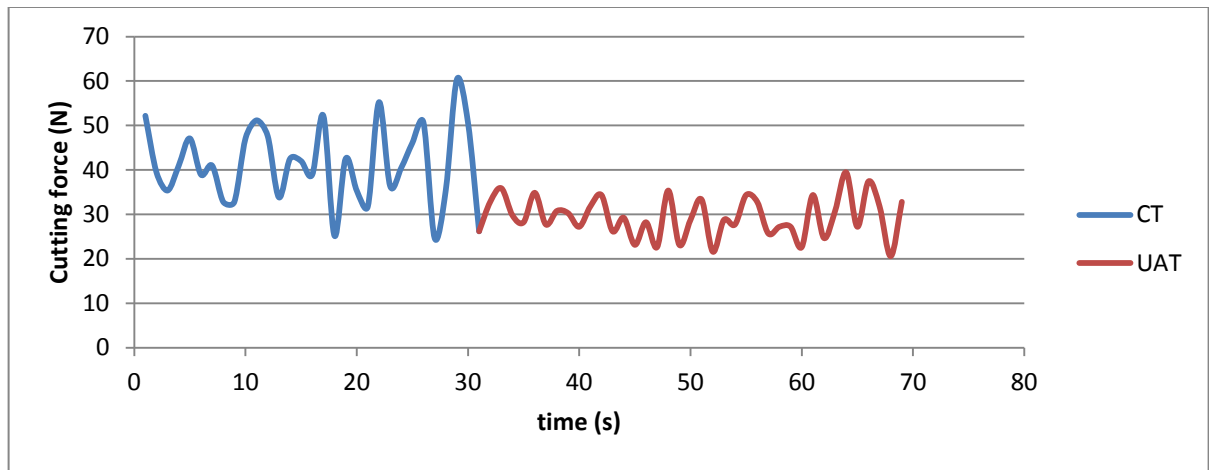


(b)

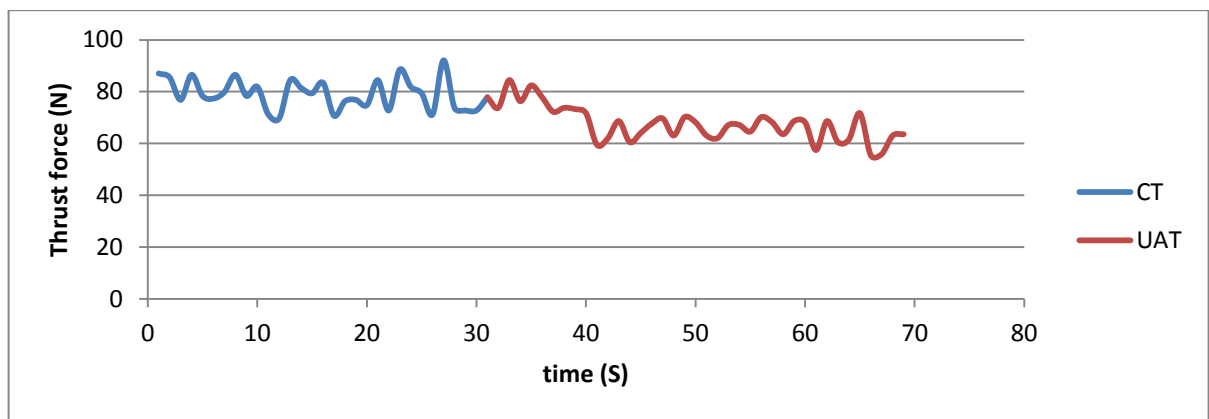


(c)

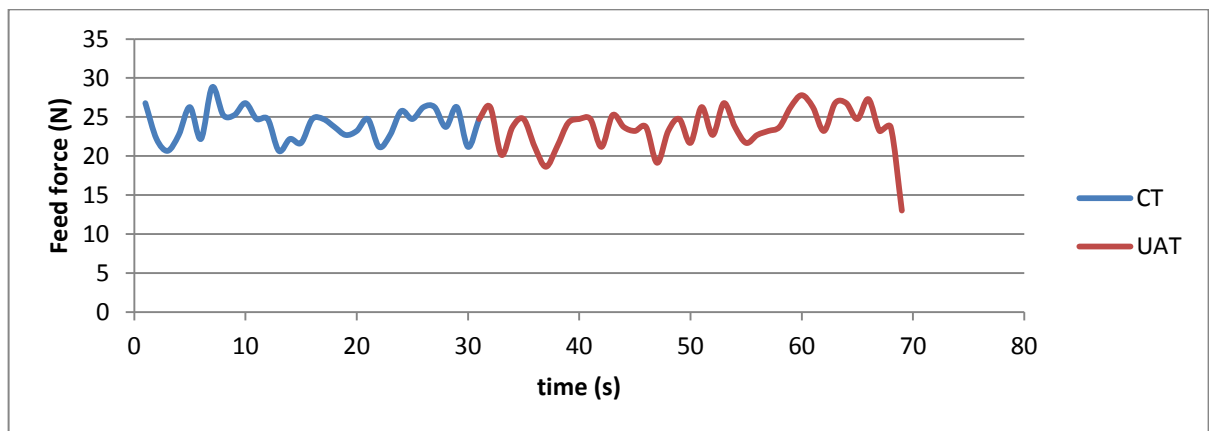
**Figure 4.8** Graph plotted between (a) cutting forces vs. time, (b) Thrust force vs. time, (c) Feed force vs. time for 4<sup>th</sup> run as defined in Table 4.4



(a)

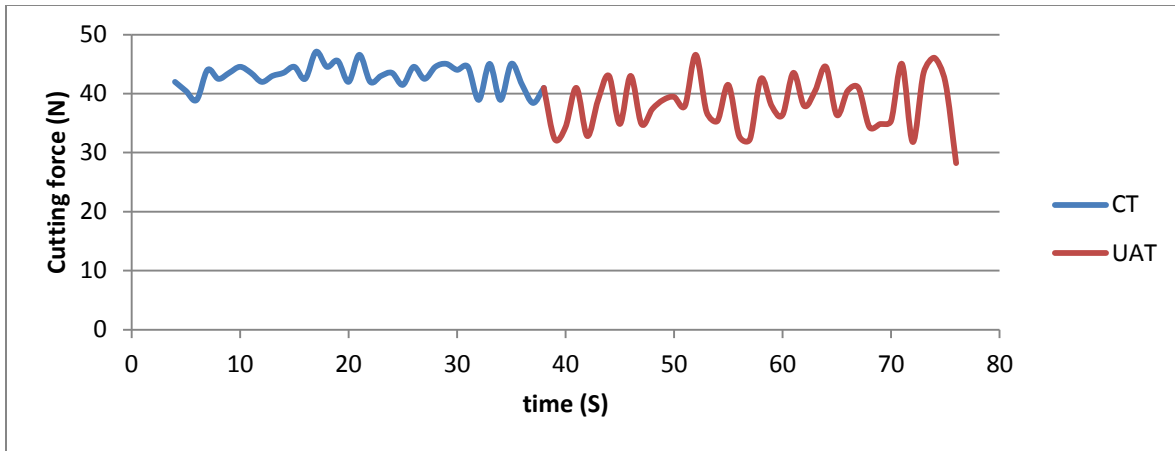


(b)

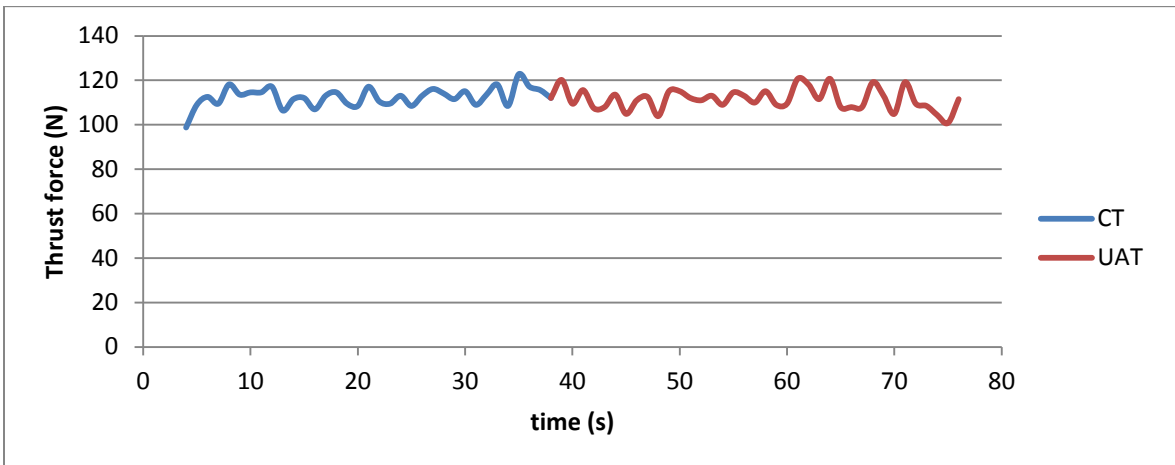


(c)

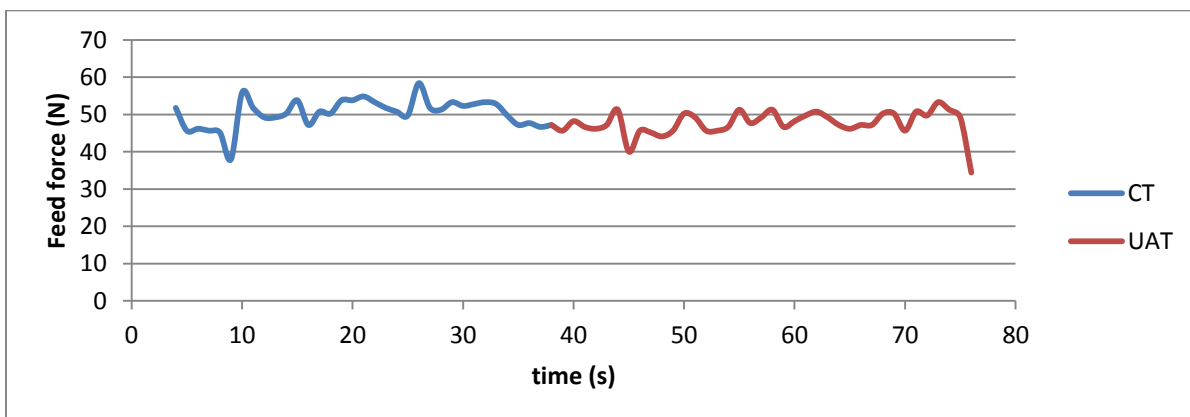
**Figure 4.9** Graph plotted between (a) Cutting force vs. time, (b) Thrust force vs. time, (c) Feed force vs. time for 5th run as defined in Table 4.4



(a)

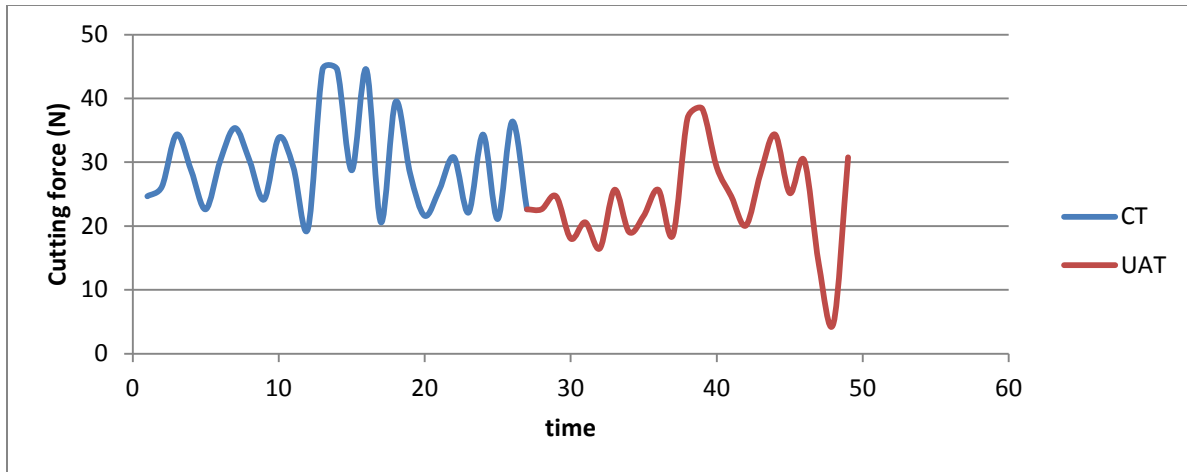


(b)

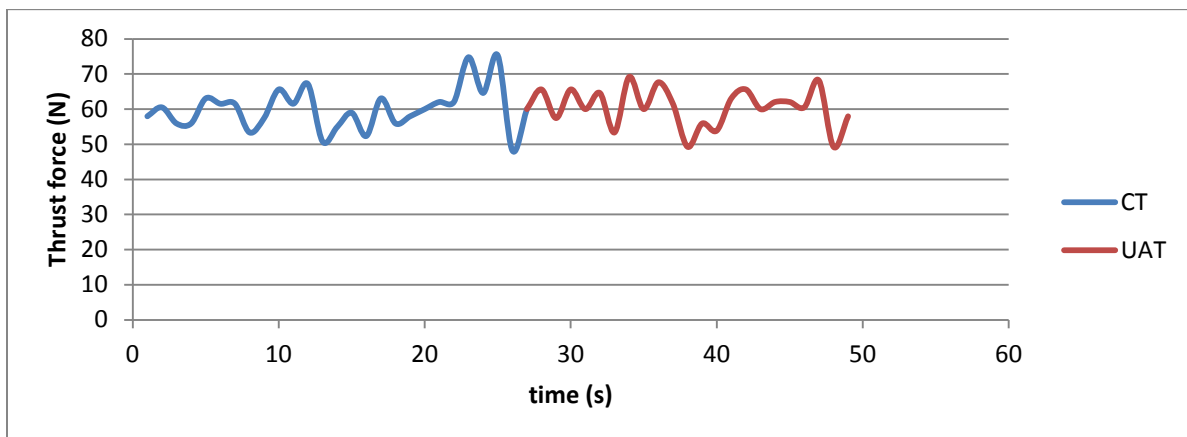


(c)

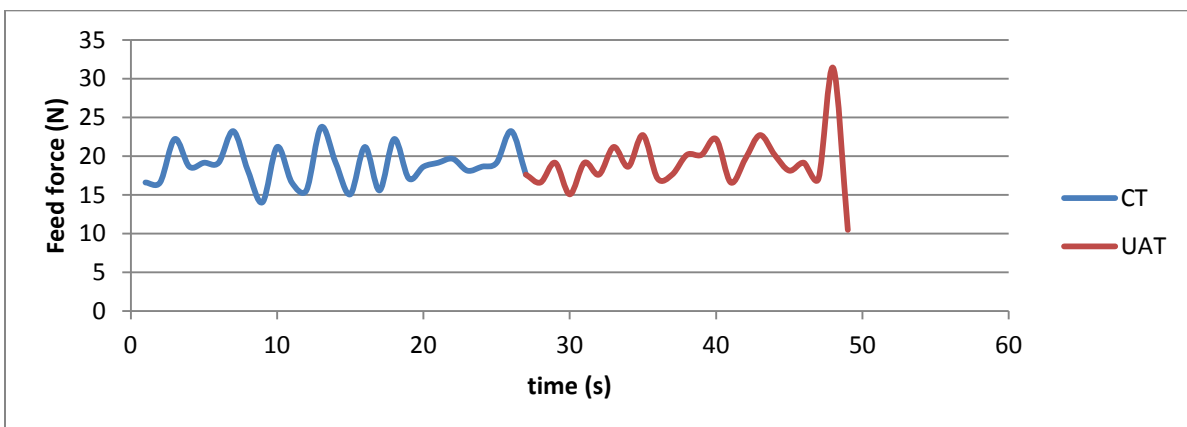
**Figure 4.10** Graph plotted between (a) cutting force vs. time, (b) Thrust force vs. time, (c) Feed force vs. time for 6<sup>th</sup> run as defined in Table 4.4



(a)

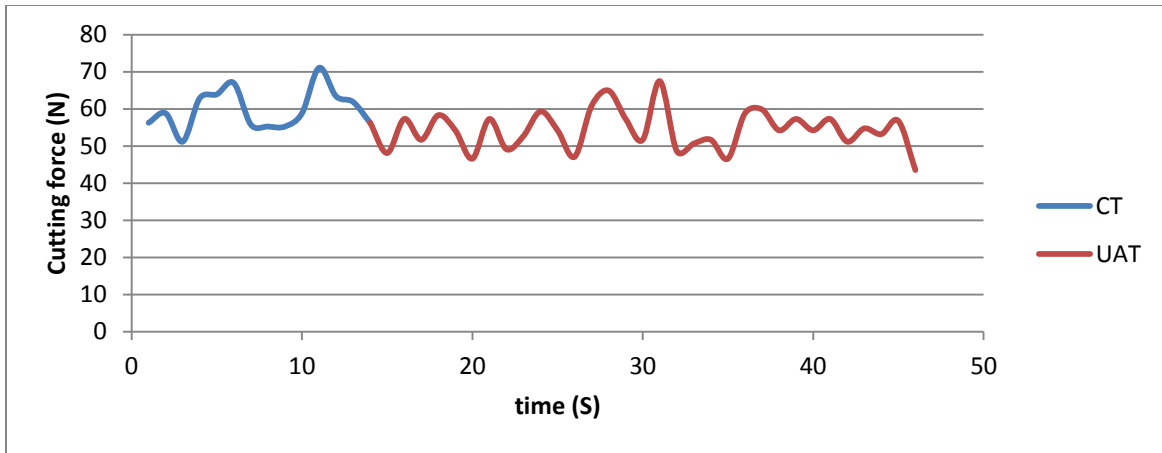


(b)

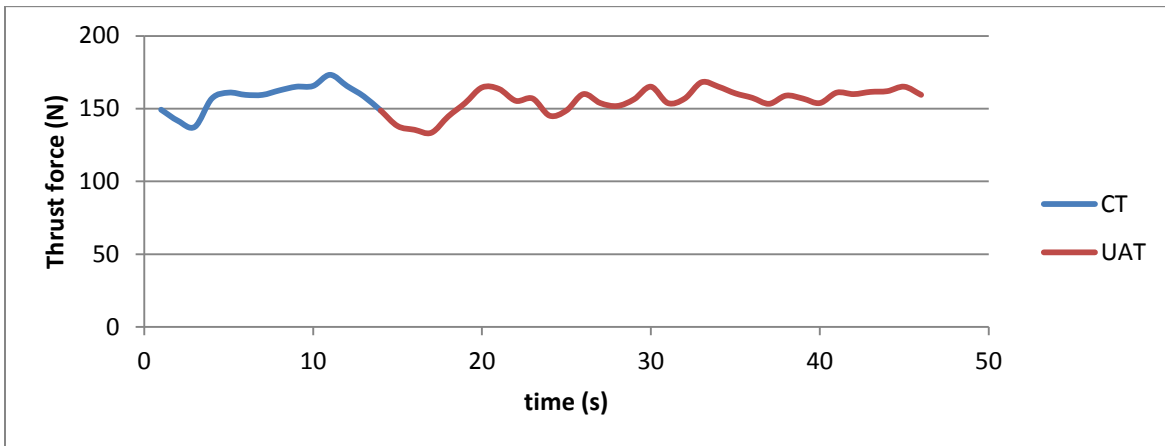


(c)

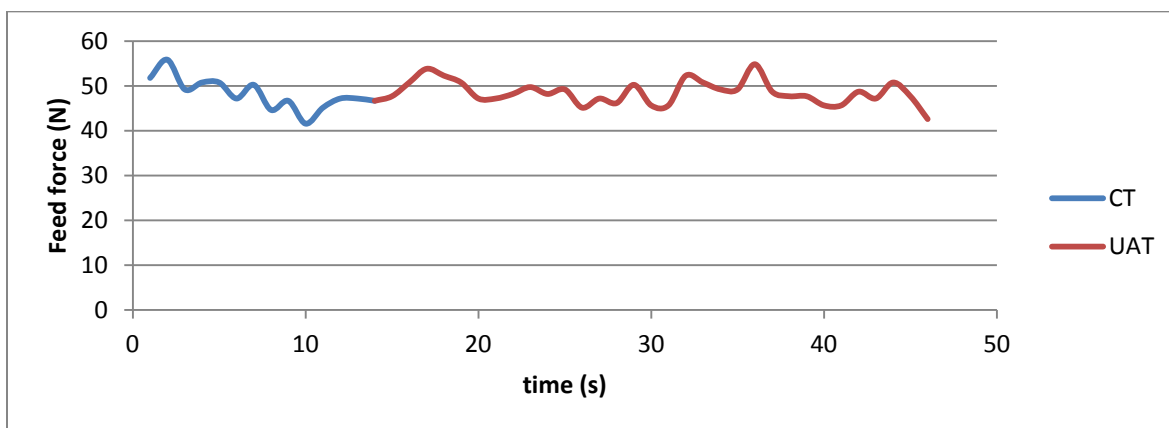
**Figure 4.11** Graph plotted between (a) cutting force vs. time, (b) Thrust force vs. time, (c) Feed force vs. time for 7<sup>th</sup> run as defined in Table 4.4



(a)

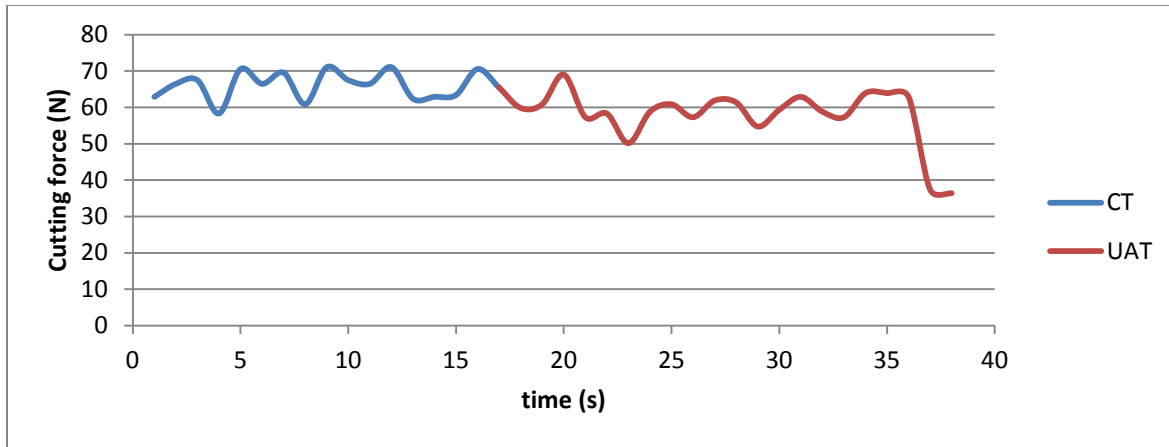


(b)

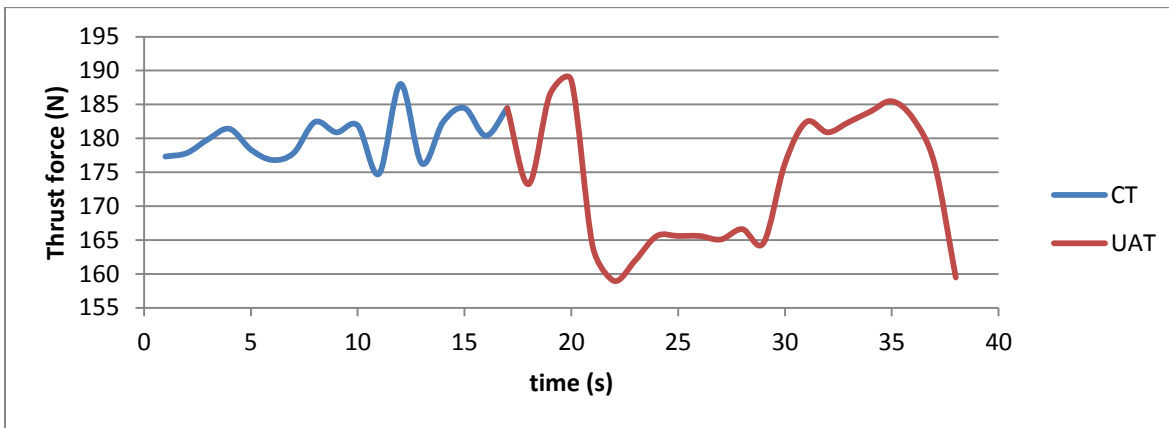


(c)

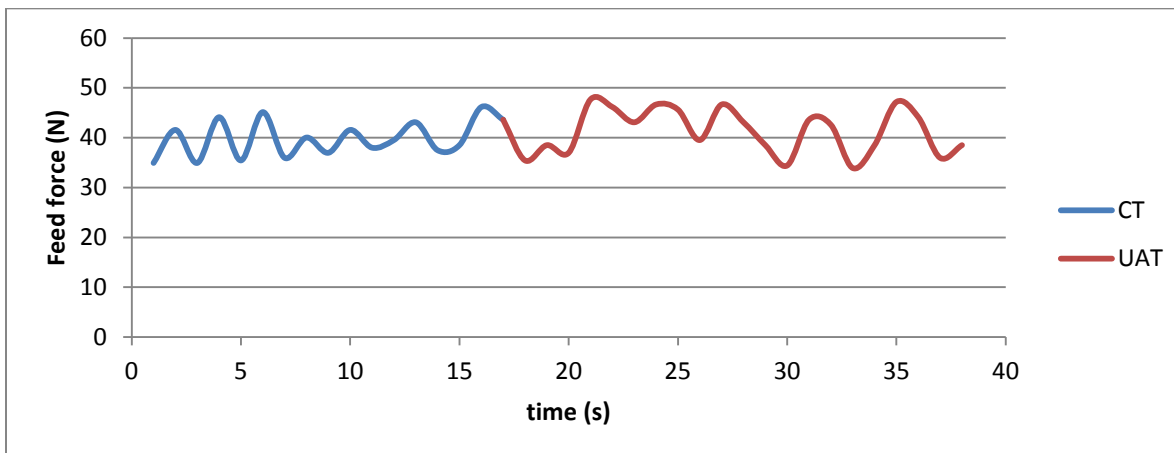
**Figure 4.12** Graph plotted between (a) cutting force vs. time, (b) Thrust force vs. time, (c) Feed force vs. time for 8<sup>th</sup> run as defined in Table 4.4



(a)



(b)

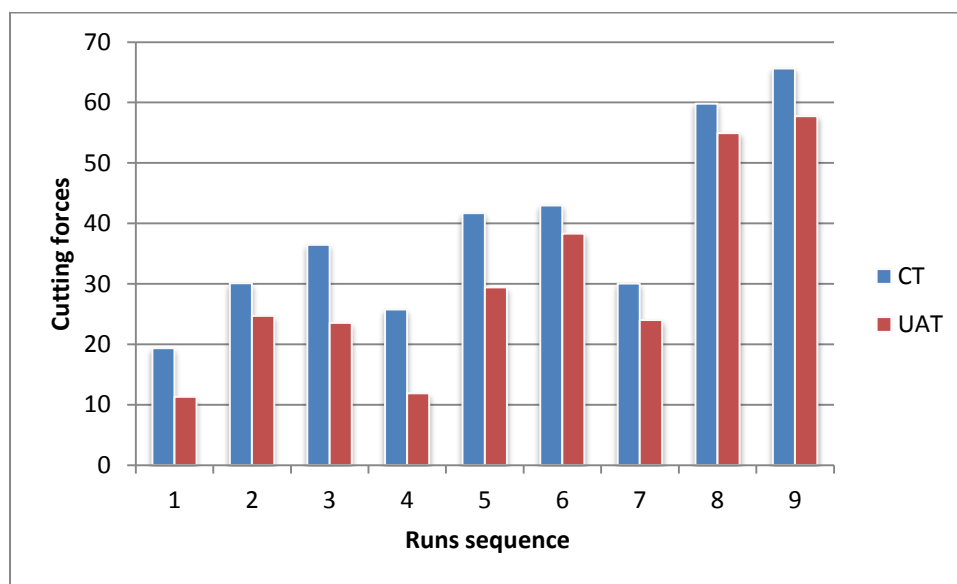


(c)

**Figure 4.13** Graph plotted between (a) cutting force vs. time, (b) Thrust force vs. time, (c) Feed force vs. time for 9<sup>th</sup> run as defined in Table 4.4

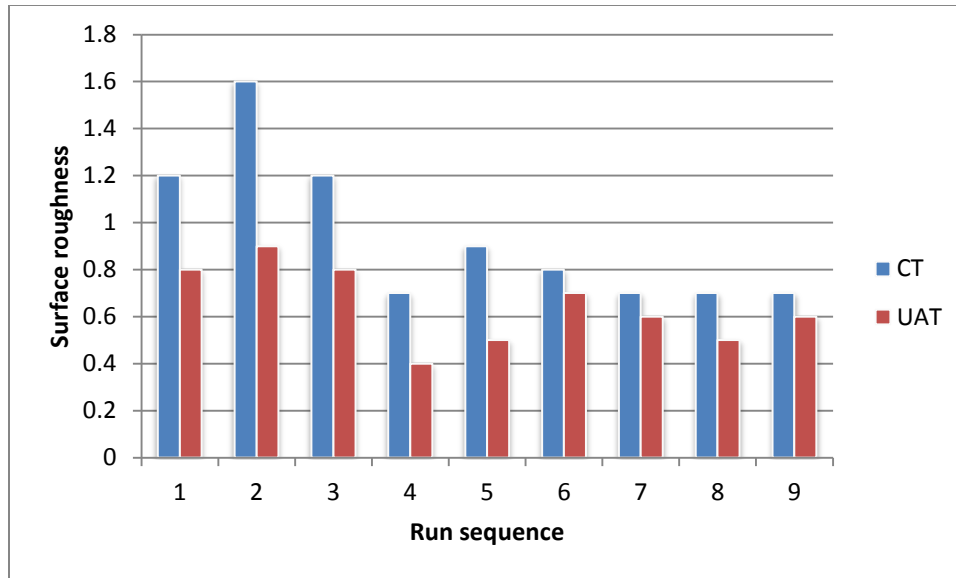


If we observed all the graphs, the average cutting force induced by UAT is reduced as compared to CT. For 1<sup>st</sup> run 41.6%, for 2<sup>nd</sup> run 17.9%, for 3<sup>rd</sup> run 35.4%, for 4<sup>th</sup> run 53.89%, for 5<sup>th</sup> run 29.46%, for 6<sup>th</sup> run 10.8%, for 7<sup>th</sup> run 20.13%, for 8<sup>th</sup> run 8.16% and for 9<sup>th</sup> run 10.07% Cutting force reduced compared to respective forced induced in CT. So overall we can conclude that as the speed increases the ultrasonic vibration to the tool having less effect on machining. Figure 4.14 shows the bar chart of CT and UAT induced force comparison. So UAT gives better result for moderate speed of operation.



**Figure 4.14** Comparison of cutting forces for each run defined in Table 4.4

Using UAT not only the cutting force decrease but also we can achieve lower surface roughness compared to CT. Figure 4.15 shows the reduction of surface roughness for each run. For 1<sup>st</sup> run surface roughness reduced by 33.3%, for 2<sup>nd</sup> run 43.75%, for 3<sup>rd</sup> run 33.3%, for 4<sup>th</sup> run 42.85%, for 5<sup>th</sup> run 44.4%, for 6<sup>th</sup> run 12.5%, for 7<sup>th</sup> run 14.3%, for 8<sup>th</sup> run 54.5% and for 9<sup>th</sup> run 14.3% observed. As we increase the cutting speed Surface roughness decreasing and it satisfy the theoretical concept.



**Figure 4.15** Comparison of surface roughness for each run defined in Table 4.4

# **CHAPTER 5**

- **Multi objective optimization**
- **Conclusion**

## 5 OPTIMIZATION OF MACHINING PARAMETER

---

### 5.1 Design of Experimentation

In the present work, experiment is conducted to optimize the machining process parameters to achieve the response to minimize. In present experiment three input process parameters are taken to minimize both Cutting force and Surface roughness. Experiment is conducted based on orthogonal array Taguchi  $L_9$  design.

Objectives of the optimization are

- To perform multi objective optimization (minimize both Cutting force and Surface roughness) to optimize process parameters for CT and UAT.
- Comparison of both optimization CT and UAT

### 5.2 Taguchi Methodology

Taguchi method is a statistical model based on orthogonal array on which the experiments give a reduced variance with optimum setting of input parameters. Orthogonal arrays gives a set up well experiments and ‘Signal to noise ratios’ which is a log functions of the desired response serves the objective function for the optimization. It can be used for both Single and Multi objective optimization.

#### 5.2.1 Gray relation grade

Since the main motive is to perform multi objective optimization, Taguchi method can't put directly to get the result. So before Taguchi method some calculation needed to perform multi objective optimization. Gray relational analysis is the simple method to convert the multiple objective responses into single objective response and perform the Taguchi method to optimize the process parameters. In the gray relational grade analysis, gray relational generation has done by normalize the individual response into 0 to 1. Normalization is calculated based on three criteria namely ‘Larger is better’, ‘Lower is better’ and ‘nominal is better’.

For Lower is better following formula is used to calculate normalize value

$$X_i(k) = \frac{\max Y_i(k) - Y_i(k)}{\max Y_i(k) - \min Y_i(k)} \quad 5.1$$

For higher is better following formula is used to calculate normalize value

$$X_i(k) = \frac{Y_i(k) - \min Y_i(k)}{\max Y_i(k) - \min Y_i(k)} \quad 5.2$$

Where  $X_i(k)$  is the Normalize value of the corresponding response

Max  $Y_i(k)$  is the maximum response obtained in the total response

Min  $Y_i(k)$  is the minimum response obtained in the total response

After finding normalized value Gray relation coefficient is calculated by following formula

$$\psi_i(k) = \frac{\Delta_{\min} + \psi \Delta_{\max}}{\Delta 0_i(k) + \psi \Delta_{\max}} \quad 5.3$$

Where  $\psi_i(k)$  is the Gray relation coefficient of  $k$ th response and  $\Delta 0_i(k)$  is the absolute value of the difference of  $X_0(k)$  and  $X_i(k)$ .

After finding Gray relational coefficient, by taking average of the corresponding responses Gray relation coefficient, Gray relational grade is calculated.

### 5.3 Multi Objective Optimization of CT

In the present experiment 3 factor 3 levels has been conducted and two responses recorded for the analysis. Table 4.3 describing the 3 factor and 3 levels values taken for experimentation. Table 5.1 gives the result of gray relational grade.

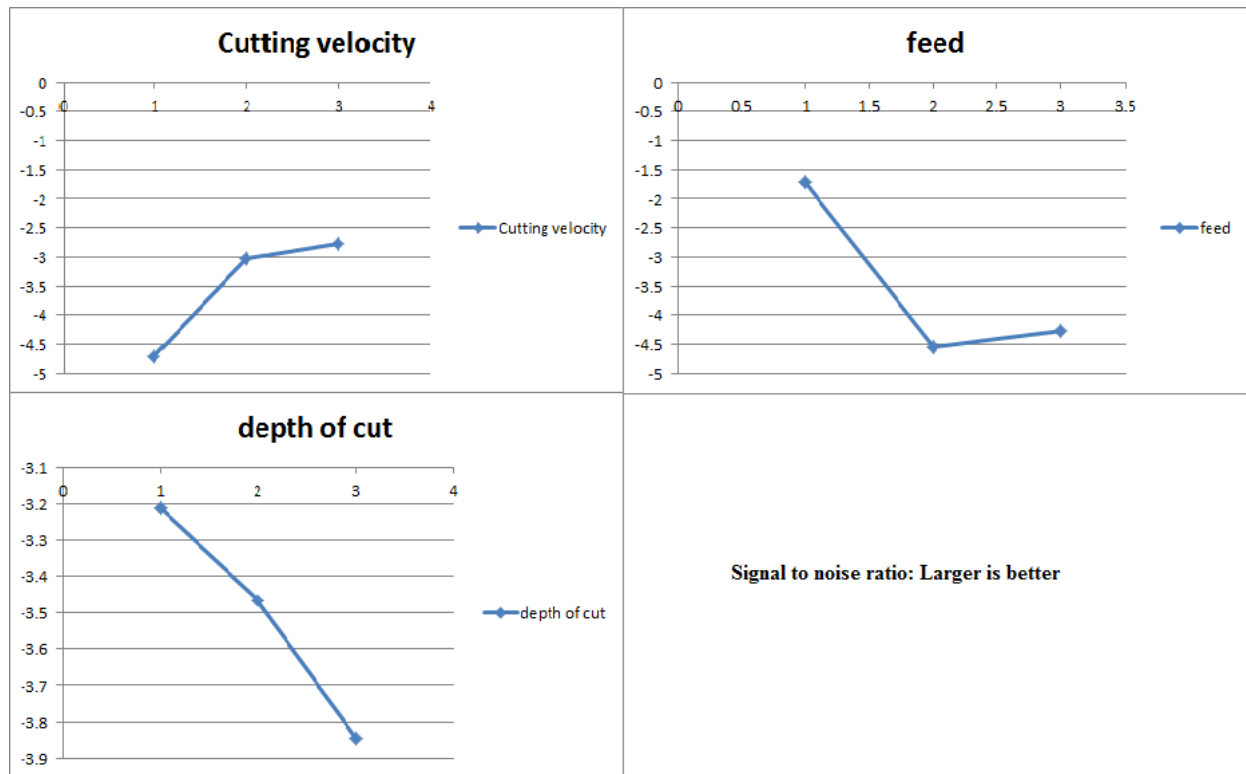
**Table 5.1** Finding Gray relational grade (GRG) for CT

no of Run	CT CF (N)	CT SR(Ra)	CF1	SR1	CF2	SR2	CF3	SR3	CT GRG
1	19.336	1.2	1	0.444444	0	0.555556	1	0.473684	0.736842
2	30.085	1.6	0.76788	0	0.23212	1	0.682948	0.333333	0.508141
3	36.477	1.2	0.629848	0.444444	0.370152	0.555556	0.574612	0.473684	0.524148
4	25.763	0.7	0.861212	1	0.138788	0	0.782732	1	0.891366
5	41.682	0.9	0.517448	0.777778	0.482552	0.222222	0.508879	0.692308	0.600593
6	42.995	0.8	0.489095	0.888889	0.510905	0.111111	0.494606	0.818182	0.656394
7	30.067	0.7	0.768269	1	0.231731	0	0.683311	1	0.841656
8	59.83	0.7	0.125551	1	0.874449	0	0.363782	1	0.681891
9	65.644	0.7	0	1	1	0	0.333333	1	0.666667

CF1 and SR1 are the Normalize values of corresponding Cutting force and Surface roughness by using lower is better formula given in equation 5.1 for CT. CF2 and SR2 are the  $\Delta 0_i(k)$  calculation for both Cutting force and surface roughness for CT. CF3 and SR3 are the Gray relational coefficient calculated by using equation 5.3 for CT. CT GRG is the Gray relation grade which is the conversion of multi objective into single objective response. The Taguchi method is applied to optimize the process parameter. Table 5.2 gives the ANOVA for CT gray relation grade.

**Table 5.2** ANOVA for CT gray relation grade

Source	DF	Seq SS	Adj SS	Adj MS	F	P
A	2	0.035875	0.035875	0.017937	18.96	0.05
B	2	0.094696	0.094696	0.047348	50.05	0.02
C	2	0.002429	0.002429	0.001214	1.28	0.438
Error	2	0.001892	0.001892	0.000946		
Total	8	0.134892				



**Figure 5.1** Main effects plot for SN ratios of CT GRG

### 5.3.1 Results and discussion

From the CT optimization analysis we found from the Table 5.2, Feed has higher significant effect to minimize both cutting force and surface roughness. Then speed has significant effect and depth of cut has very less significant effect to minimize both cutting force and surface roughness. The model has high determination coefficient R-Sq 98.60% and R-Sq (adj) 94.39%, which indicates the goodness fit for the model and having higher significance. From Figure 5.1 the optimize parameters are 3-1-1 levels means higher speed, lower feed and lower depth of cut. It is quite obvious that both cutting force and surface roughness improves on higher cutting speed and low feed and depth of cut which matches the theoretical concepts.

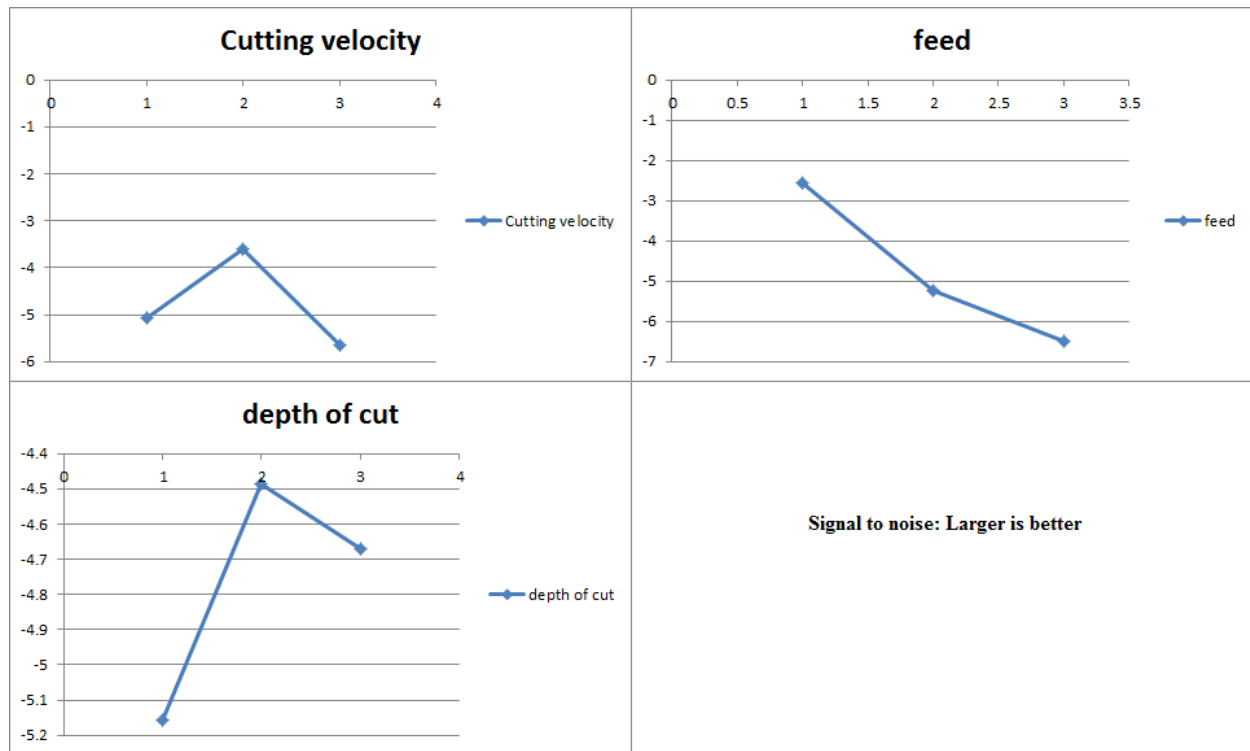
### 5.4 Multi Objective Optimization of UAT

Similarly multi objective optimization has been done for UAT. Table 5.3 gives the Gray relational grade for UAT to make it single response.

**Table 5.3** Gray relation grades for UAT

no of Run	UAT CF (N)	UAT SR (Ra)	CF1	SR1	CF2	SR2	CF3	SR3	GRG
1	11.289	0.8	1	0.2	0	0.8	1	0.384615	0.692308
2	24.688	0.9	0.711713	0	0.288287	1	0.634287	0.333333	0.48381
3	23.549	0.8	0.736219	0.2	0.263781	0.8	0.654638	0.384615	0.519627
4	11.878	0.4	0.987327	1	0.012673	0	0.975281	1	0.987641
5	29.399	0.5	0.610353	0.8	0.389647	0.2	0.562021	0.714286	0.638153
6	38.326	0.7	0.418284	0.4	0.581716	0.6	0.462228	0.454545	0.458387
7	24.014	0.6	0.726215	0.6	0.273785	0.4	0.646174	0.555556	0.600865
8	54.942	0.5	0.060781	0.8	0.939219	0.2	0.347411	0.714286	0.530848
9	57.767	0.6	0	0.6	1	0.4	0.333333	0.555556	0.444444

CF1 and SR1 are the Normalize values of corresponding Cutting force and Surface roughness by using lower is better formula given in equation 5.1 for UAT. CF2 and SR2 are the  $\Delta 0_i(k)$  calculation for both Cutting force and surface roughness for UAT. CF3 and SR3 are the Gray relational coefficient calculated by using equation 5.4. GRG is the Gray relation grade which is the conversion of multi objective into single objective response for UAT. The Taguchi method is applied to optimize the process parameter. Table 5.4 gives the ANOVA for UAT gray relational grade.



**Figure 5.2** Main effects plot for SN ratios of UAT

**Table 5.4** ANOVA for UAT Gray relation grade

Source	DF	Seq SS	Adj SS	Adj MS	F	P
A	2	0.04703	0.04703	0.02352	1.15	0.465
B	2	0.13158	0.13158	0.06579	3.22	0.237
C	2	0.00951	0.00951	0.00476	0.23	0.811
Error	2	0.0409	0.0409	0.02045		
Total	8	0.22902				

#### 5.4.1 Result and discussion of UAT

From the analysis we found that, neither of these parameters having significant effect according to the calculation but we know that speed, feed and depth of cut has some significant effect. The UAT multi optimization model has presented  $R^2$  82.14%. From the Gray Taguchi optimization 2-1-2 levels means cutting speed of 38.48 m/min, feed 0.06 mm/rev and depth of cut 0.2 mm gives good results as shown in Figure 5.2. It is showing the different path because, the cutting velocity may approach or closer to the vibration velocity which is explain in equation 1.1 [5]. Good number of experiment needed to get the better result.



## 5.5 Conclusion

Multi objective optimization is performed for both CT and UAT by using Taguchi methodology. From the multi objective optimization following conclusion made.

- For CT the optimize process parameters found in 3-1-1 levels means Cutting velocity level 3 (65.97 m/min), feed level 1 (0.06 mm/rev) and depth of cut 0.15 mm. It is matching the theoretical concept because at the higher cutting speed, lower feed and lower depth of cut we can get good surface finish and lower cutting force.
- But UAT optimization is showing different path. In the UAT multi optimization, the optimize parameters found in 2-1-2 levels. The 2-1-2 levels present in the Run no 4, so no need for conducting confirmatory test. It may come because of the cutting velocity closer to vibration velocity (equation 1.1) [5]. Good number of experiment will give better result.
- Confirmatory test has been done for CT in level 3-1-1 to ensure that the analysis has done correctly. And we found the Cutting force 27.684 N and roughness 0.7 having SN ratio -1.23 which is close to -0.69.

# **CHAPTER 6**

- **CONCLUSIONS**
- **FUTURE RECOMMENDATIONS**

## 6 CONCLUSIONS AND FUTURE RECOMMENDATIONS

---

### 6.1 Conclusions

In the present research the whole concept has been divided into three major parts. One is FEM analysis of the total Horn-tool assembly to know the behavior of the horn under dynamic load, second is Experimental investigation of the CT and UAT machining process and finding the difference between them in terms of induced forces and surface roughness generated and third one is the multiple objective optimization of CT and UAT to finding optimize parameters to minimize both cutting force and surface roughness. From the above whole observation following conclusion has been made.

- FEM analysis has been done for the horn assembly by using ANSYS® software. The analysis has two parts. One is Modal analysis and the other one is Harmonic analysis. The stepped horn having 126 mm of length, input diameter 40 mm, output diameter 20 mm, fillet of 2 mm radius and made of mild steel connected with tool insert having 5 mm thickness by screw is designed in SOLIDWORK software and import onto the ANSYS® software.
- In Modal analysis, 19925.5 Hz natural frequency has found for the whole assembly in 1<sup>st</sup> node only and from Harmonic analysis it is found that the amplitude of vibration at the output end is approximately 4 times amplitude of vibration of input end which is satisfy the theoretical concept.
- From the experimental investigation it is found that, the cutting force reduced by 8.16% to 53.89% and the surface roughness reduced by 12.5% to 54.5%. The feed and thrust force is approximately same for CT and UAT. So UAT is suitable process for machining hard material as compared to CT. As we increase the cutting speed both the cutting force and surface roughness reduced and at a certain speed at which the cutting speed equal to amplitude vibration speed, UAT is not recommended for the machining.
- Multi objective optimization is performed using Gray Taguchi method for both CT and UAT. For CT 3-1-1 levels giving the better result which is quite obvious that at higher cutting speed and low feed and depth of cut, we will get low cutting force and low surface roughness. In UAT process 2-1-2 levels find better result. It may happen due to

the cutting velocity closer to vibration velocity of the horn which causes no vibration effect to machining process similar to CT.

## **6.2 Future Recommendations**

- Further investigation required for tool insert wear rate, effect of tool angles (rake angle, nose radius).
- Further analysis required for chip produced by UAT and CT process to find theoretical force calculation, stress and strain generation.
- Further investigation required for the effect of different horn material on machining process for different work piece materials.
- Further investigation required for different direction of vibration cutting.

# **REFERENCES**

## REFERENCES

---

- [1] Astashev V.K, Effect of ultrasonic vibrations of a single point tool on the process of cutting, *J. Mach. Manuf. Reliability*, 5 (3), 1992, pp. 65–70.
- [2] Morowaki T., E. Shamoto and K. Inoue, Ultraprecision ductile cutting of glass by applying ultrasonic vibration, *CIRP Annals*, 1992, 41(1), pp. 559-562.
- [3] Xiao M., Sato K., Karube S. and Soutome T. The effect of tool nose radius in ultrasonic vibration cutting of hard material, *International Journal of Machine Tools and Manufacture*, Volume 42 (2002): pp. 1377-1385
- [4] Kumabe J. *Vibratory cutting*, Tokyo(in Japanese), 1979
- [5] Astashev V. K. and Babitsky V. I. Ultrasonic cutting as a nonlinear (vibro-impact) process, *Ultrasonics*, 36 (1998): pp. 89-96.
- [6] Devin j. Ultrasonically assisted metal removal, *SAMPLE Quarterly*, 10 (1979): pp. 485-496.
- [7] Takeyama H. and Iijima. Machinability of glass fiber reinforced plastics and application of ultrasonic machining, *Annals CIRP*, 37(1) (1988): pp. 93-96.
- [8] Kremer D. Ultrasonically assisted machining, *Mech. Ind. Mater.*, 48(1) (1995): pp.15-21.
- [9] Ahmed N., Mitrofanov A.V., Babitsky V.I., Silberschmidt V.V. Analysis of forces in ultrasonically assisted turning, *Journal of Sound and Vibration*, Vol. 308 ( 2007): pp. 845-854
- [10] Sharma V.S., Dogra M. and Suri N.M. Advance in the turning process for productivity improvement, *JEM*, Volume 222 (2008): pp. 1417-1441
- [11] Nath C. and Rahman M. Effect of machining parameters in ultrasonic vibration cutting, *International Journal of Machine Tools and Manufacture*, Vol. 48 (2008): pp. 965-974
- [12] Amini S., Soleimanimehr H., Nategh M.J., Abudollah A. and Sadeghi M.H. FEM analysis of ultrasonic assisted turning and the vibratory tool, *Journal of Material Processing Technology*, Vol. 20 (2008): pp. 43-47
- [13] Mitrofanov A.V., Babitsky V.I. and Silberschmidt V.V. Finite element analysis of ultrasonically assisted turning of Inconel 718, *Journal of Materials Processing Technology*, Vol. 153-154 (2004): pp. 233-239
- [14] Seah K.H.W., Wong Y.S. and Lee L.C. Design of tool holders for ultrasonic machining using FEM, *Journal of Materials Processing Technology*, Vol. 37 (1993): pp. 801-816

- [15] Ahmed N., Mitrofanov A.V., Babitsky V.I., Silberschmidt V.V. 3D finite element analysis of ultrasonically assisted turning, *Computational Materials Science*, Volume 39 ( 2007): pp. 149-154
- [16] Celaya A., Lacalle L., Campa F.J. and Lamikiz A. Ultrasonic assisted turning of mild steels, *Int. J. Materials and Product Technology*, Vol. 37 (2010): pp. 60-70
- [17] Nad M. Ultrasonic horn design for ultrasonic machining technologies, *Applied and Computational Mechanics*, Vol. 4 (2010): pp. 79-88
- [18] Babitsky V.I., Kalashnikov A.N., Meadows A. and Wijesundara A.A.H.P. Ultrasonically assisted turning of aviation materials, *Journal of Materials Processing Technology*, Vol. 132 (2003): pp. 157-167
- [19] Akbari J., Chegini A.G. and Rajabanejad A.R. Ultrasonic assisted turning NiTi shape Memory alloy, *International Conference and Exhibition on Design and Production of Machines and Dies/Molds*, (2009)
- [20] Muhammad R., Maurotto A., Demiral M., Roy A. and Silberschmidt V.V. Thermally enhanced ultrasonically assisted machining of Ti alloy, *CIRP Journal of Manufacturing Science and Technology*, (2014): pp. 265-273
- [21] Dong G., Zhang H., Zhou M. and Zhang Y. Experimental Investigation on ultrasonic vibration assisted turning of SiCp/Al composites, *Materials and Manufacturing Processes*, Vol. 28 (2013): pp. 999-1002
- [22] Thoe T.B., Aspinwall D.K. and Wise M.L.H. Review on ultrasonic machining, *Int. J. Mach. Tools Manufact*, vol. 38, No. 4 (1998): pp. 239-255
- [23] Amin S., Khosrojerdi M.R., Nosouhi R. and Behbahani S. An experimental investigation on the machinability of  $Al_2O_3$  in vibration assisted turning using PCD tool, *Materials and Manufacturing Processes*, Vol. 29 (2014): pp. 331-336
- [24] Nanu A.S., Marinescu N. I. and Ghiculescu D. Study of ultrasonic stepped horn geometry design and FEM simulation, *Nonconventional Technologies Reviews*, Vol. 4 (2011): pp. 25-30